Montoya, V., Noseck, U., Mattick, F., Britz, S., Blechschmidt, I., Schäfer, T. (2022):
Radionuclide geochemistry evolution in the Long-term In-situ Test (LIT) at Grimsel Test Site (Switzerland)
J. Hazard. Mater. **424, Part D** , art. 127733

http://dx.doi.org/10.1016/j.jhazmat.2021.127733

Radionuclide geochemistry evolution in the Long-term In-situ Test (LIT) at Grimsel Test Site (Switzerland)

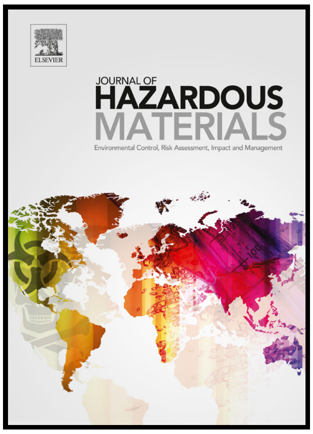

Vanessa Montoya, Ulrich Noseck, Felix Mattick, Susan Britz, Ingo Blechschmidt, Thorsten Schäfer

PII: S0304-3894(21)02702-3
DOI: https://doi.org/10.1016/j.jhazmat.2021.127733
Reference: HAZMAT127733

To appear in: *Journal of Hazardous Materials*

Received date: 27 August 2021
Revised date: 4 November 2021
Accepted date: 5 November 2021

Please cite this article as: Vanessa Montoya, Ulrich Noseck, Felix Mattick, Susan Britz, Ingo Blechschmidt and Thorsten Schäfer, Radionuclide geochemistry evolution in the Long-term In-situ Test (LIT) at Grimsel Test Site (Switzerland), *Journal of Hazardous Materials,* (2021) doi:https://doi.org/10.1016/j.jhazmat.2021.127733

Radionuclide geochemistry evolution in the Long-term In-situ Test (LIT) at Grimsel Test Site (Switzerland)

Vanessa Montoya[1,2, *], *Ulrich Noseck*[3] , *Felix Mattick*[2], *Susan Britz*[3], *Ingo Blechschmidt*[5], *Thorsten Schäfer*[2,4]

[1] Department of Environmental Informatics – Helmholtz Centre for Environmental Research (UFZ), 04318, Leipzig, Germany

[2] Institute for Nuclear Waste Disposal (INE), Karlsruhe Institute of Technology (KIT), 76021, Karlsruhe, Germany

[3] Gesellschaft für Anlagen- und Reaktorsicherheit (GRS), 38122, Braunschweig, Germany

[4] Friedrich-Schiller-University Jena (FSU), Institute of Geosciences – Applied Geology, 07749, Jena, Germany

[5]Nagra (National Cooperative for the Disposal of Radioactive Waste) 5430 Wettingen, Switzerland

*Corresponding author: Vanessa Montoya (vanessa.montoya@ufz.de) Postal-address: Helmholtz Centre for Environmental Research, Permoserstraße 15, 04318, Leipzig, Germany

Abstract

The Long-term In-situ Test (LIT) of the Colloid Formation and Migration project (CFM) at the Grimsel Test Site, investigates the generation of bentonite colloids and, hence, radionuclide mobilization within a well-defined and controlled shear zone in a crystalline rock. In this context, the determination of radionuclide aqueous speciation is essential to understand whether radionuclides are easily transported or immobilized by precipitation or uptake processes in the bentonite barrier included in a repository concept for nuclear waste, and mimic in the LIT experiment. The objective of this work is to determine the aqueous speciation of seven radionuclides (i.e. ^{75}Se(VI), ^{99}Tc(VII),^{233}U(VI), ^{237}Np(V), ^{241}Am(III), Th(IV) and ^{242}Pu(IV)) by thermodynamic calculations in different water compositions representing the geochemical evolution through the LIT. A comparison of the results obtained from two different modelling groups allows the identification of the geochemical key parameters affecting radionuclide mobility in this context and the corresponding numerical and conceptual uncertainties. Particularly, silicate complexes of trivalent actinides and uranium(VI) carbonato complexes (i.e. $Ca_nUO_2(CO_3)_3^{(4-2n)}$) seem to be crucial in these environments, even at reducing conditions. Conceptual uncertainties like inclusion/exclusion of tetravalent actinide-bearing colloids formation and polyselenides have clearly been identified.

Graphical Abstract

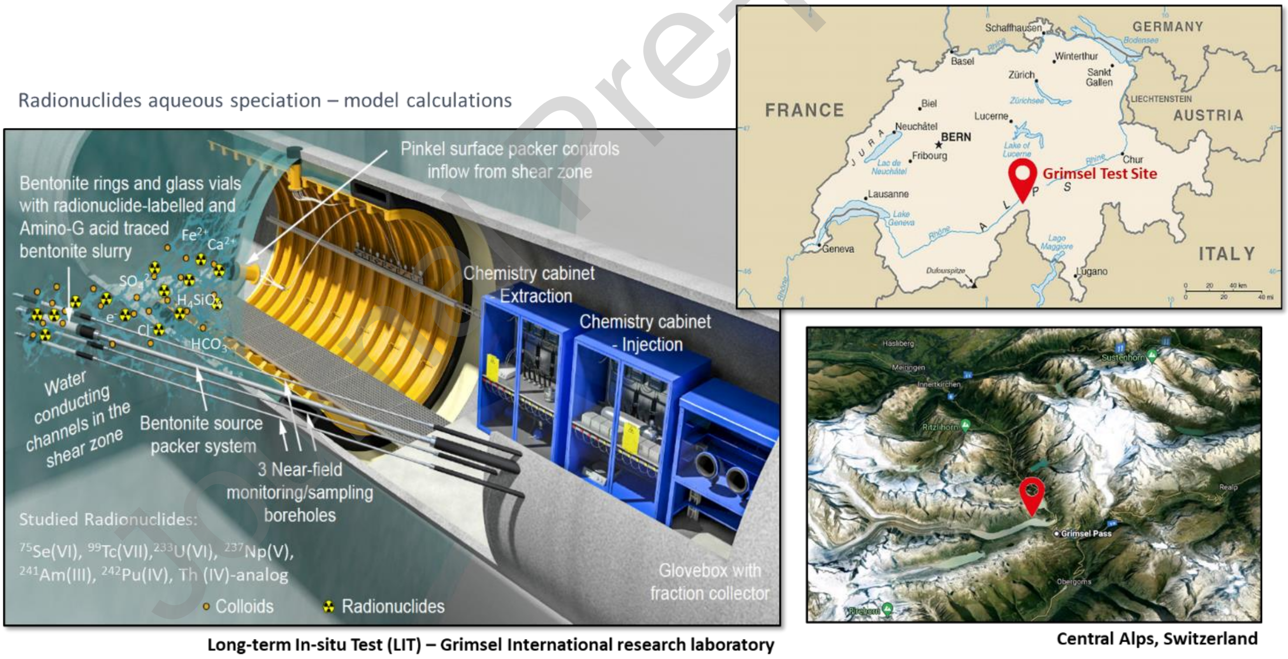

KEYWORDS:

Grimsel Test Site, radionuclides speciation, solubility, thermodynamic databases, benchmark, FEBEX bentonite

1. INTRODUCTION

The influence of colloidal/nanoparticulate phases on radionuclide (RN) mobility as well as long-term erosion rates of the geo-engineered barrier compacted bentonite under glacial melt water conditions in crystalline environments still represent uncertainties in repository safety assessments in countries like UK, China, Russia, Japan, Korea, Spain, Canada, Czech Republic, or Germany (Kurosawa and Ueta, 2001; Alonso et al., 2006, Novikov et al. 2006; Baik et al. 2008; Nykyri et al., 2008; SKB, 2011; Kelly et al., 2012; Schäfer et al., 2012; Sellin and Leupin, 2013; Kolomá et al., 2018, Shelton et al., 2018; Xu et al. 2020; Hoyer et al., 2021). Within the Colloid Formation and Migration (CFM) project at the Grimsel Test Site (GTS, Switzerland) a hydraulically controlled natural shear-zone was utilized to simulate a deep geological nuclear waste disposal post-closure situation in crystalline rock (Schlickenrieder et al. 2017). Within the so-called Long-term In-situ Test (LIT) of CFM a compacted FEBEX bentonite source was emplaced in this shear zone in May 2014 and labelled with RN tracers to investigate a) the engineered-barrier performance in contact with a water-conducting feature and b) the potential migration of RNs. Geochemical and hydro-mechanical parameters in LIT had been continuously monitored over 1626 days (≈ 4.5 years) until the start of the over-coring in 2018. The cocktail of eight RNs (i.e. actinides, long-lived fission and activation products, namely ^{75}Se(VI), ^{99}Tc(VII),^{137}Cs(I), ^{45}Ca(II), ^{233}U(VI), ^{237}Np(V), ^{241}Am(III) and ^{242}Pu(IV)) were introduced in a pre-defined oxidation state in the bentonite. These oxidation states are not necessarily expected under real repository conditions, but chosen to monitor near-field redox reactions and colloid associated RN transport. Low RN concentrations (10^{-5} – $4x10^{-10}$ mol L^{-1}) were carefully selected in order to avoid precipitation of any radionuclide containing solid phases through the whole range of geochemical conditions developed during the LIT and considering the sensitivity of the analytic techniques used for their analysis (i.e. ICP-MS, SF-ICP-MS, LSC, AMS and γ-spectroscopy (Quinto et al. 2017, 2019). In addition, specific isotopes such as ^{233}U were selected to avoid interferences in the measurements with naturally occurring uranium in the rock, mainly present as U-238 and in less extend U-234 (Harrison et al., 2016). During the LIT, groundwater chemistry was monitored online and regularly sampled and characterized (e.g. pH, Eh, ion concentration) from one of three near-field monitoring boreholes, drilled between 5 and 10 cm from the bentonite source interval, including colloid quantification using a mobile Laser Induced Breakdown Detection (LIBD) system (Rinderknecht et al. 2019). The controlled outflow from the shear zone was additionally monitored.

The conceptual and numerical modelling approach to simulate the colloid and associated RN transport in the LIT needs to be justified by a thorough understanding of the factors influencing RN transport and retardation processes in the bentonite. It is well known that the behavior of RNs in the environment is mainly determined by their speciation in the aquatic system given by the geochemical boundary conditions. For example, model calculations of RN diffusion in the bentonite source of the LIT indicate that tri- and tetravalent RNs are expected to be released from the bentonite source within 4.5 years of experimental duration, whereas RNs in higher oxidized states, e.g. Tc(VII), U(VI), Np(V) and Pu(V), if present, are likely to be released into the contact water (Rinderknecht et al. 2019). Speciation calculations might show that the observed decrease in recovery of uranium and neptunium with increasing transport time, within the GTS shear zone, is due to a reduction of mobile Np(V) and U(VI) to their more immobile tetravalent forms (Rinderknecht et al. 2019).

The present work provides a benchmark thermodynamic modelling exercise performed independently by two groups in the definition of the RN speciation and solubility under the geochemical boundary conditions of the LIT experiments. The methodology used by both groups is similar and follows the approximation described in Bruno et al. (2000) for a similar engineered-barrier system (i.e. FEBEX bentonite and Grimsel groundwater) studying colloid and radionuclide retardation processes. Since the earlier thermodynamic modelling benchmark in 2000 (Bruno et al. 2000), updates affecting RN speciation calculations have been reported in the literature which are mainly related to new thermodynamic data (Duro et al. 2010), more detailed knowledge on ground- and porewater compositions (Grivé et al. 2008) and redox conditions for the scenario of interest. For this reason, the comparison of the results obtained by both modeler groups allows the identification of geochemical key parameters affecting RN migration in the LIT experiments and the description of the conceptual uncertainties that significantly influence the calculation results (i.e. thermodynamic databases, water composition and/or aqueous models)

2. METHODS

2.1 Modelling approach

Calculations were undertaken using PHREEQC v.3.5 (Parkhurst and Appelo, 2013) and PhreePlot v.11, (2017 release) (Kinniburgh and Cooper, 2011) to generate Pourbaix diagrams, respectively. Aqueous speciation calculations for six of the eight RNs used in the LIT experiment (i.e. ^{75}Se(VI), ^{99}Tc(VII), ^{233}U(VI), ^{237}Np(V), ^{241}Am(III) and ^{242}Pu(IV)) have been performed by both groups. Additionally, thorium has been included in the assessment, as a redox stable analog of U, Np and Pu in their tetravalent state to facilitate the interpretation of the evolving redox conditions in the LIT experiment. The simulations consider only reactions in thermodynamic equilibrium at 25 ºC and three different groundwater compositions (i.e. bentonite porewater, Grimsel groundwater and “mixed water”) with representative redox conditions of the LIT experiment (see Table A.1 in Appendix). The composition of the Grimsel groundwater (GGW) is described in Duro et al. (2006) and Grivé et al. (2010a, 2010b) and the bentonite porewater was given in Fernandez et al. (2004). To reflect the differences between the initial conditions after emplacement of the bentonite source, when oxygen is still available, and the more reducing conditions expected to develop in the long-run of the experiment due to the existence of reducing mineral phases like pyrite and siderite a reducing and an oxidizing bentonite porewater, BPWR and BPWO, respectively, was defined. An additional water composition (“mixed waters” MWs) representing the interface between bentonite and the shear zone in the granite was calculated by both groups, for a 10/90 % mixture of BPWR and GGW, denoted as mixed water reducing (MWR) and a 10/90 % mixture of BPWO and GGW, denoted as mixed water oxidizing (MWO).

Calculated maximum concentrations and the solubility determining solid phases of the seven RNs in the five water compositions were assessed to determine if any solid phase can be formed during the LIT. These calculations were done by means of numerical increase of the aqueous RN concentrations until equilibrium was achieved between solution and the solubility-limiting solid phases, which avoids unintentional changes of the groundwater speciation, as mentioned in e.g. Bennet, (2014). According to the Ostwald’s rule, the precipitation of less crystalline phases (amorphous phases) is kinetically favored and was assumed to be formed in the studied system over crystalline phases.

2.2 Thermodynamic Databases

Two different state of the art thermodynamic databases were used in the assessment by the two different groups, although, both databases are using the NEA Thermodynamic database (TDB) project (Guillaumont et al. 2003; Olin et al. 2005; Rand et al. 2008) as a base for the thermodynamic data selection. In the last years, important updates in thermodynamic databases incorporate new aqueous species between trivalent actinides and silica (Thakur et al. 2007; Altmaier et al. 2013) and ternary Ca-U(VI)- carbonates (Dong and Brooks, 2006; Lee et al. 2019) which have shown to be relevant for radionuclide behavior in environmental systems (Reiller et al. 2012; Reiller and Descostes, 2020) and not considered in earlier studies (Bruno et al. 2000). Thermodynamic data of iron selenides solid phases have also been updated recently (Olin et al. 2005, Lemire et al. 2020). Stability constants and solubility products of the studied RNs are available in the Appendix (Table A.3.1, A.3.2, A.3.3, A.3.4, A.3.5, A.3.6, A.3.7). Specifically,

Group A used their internal database updated in 2017 (Stockmann et al. 2017), which is mainly based on the PSI/Nagra Chemical Thermodynamic Database 12/07 (PSI/Nagra TDB 12/07) (Thoenen et al. 2014). In some cases, information and data from the THEREDA database were also considered (Moog et al. 2015). The Davies equation was used for the ionic strength correction which is valid for aqueous solutions with ionic strengths < 0.5 M.

Group B used ThermoChimie v.10a database, updated in 2018 (Giffaut et al. 2014) and the Specific ion Interaction Theory (SIT) as ionic strength correction. This approximation gives good results for ionic strengths < 2 M. Additionally, polynuclear species like polyselenides were not considered in these calculations, although included in ThermoChimie database. This decision was due to the uncertain model and thermodynamic data selected for these species, for example, for Se_2^{2-}, Se_3^{2-}, and Se_4^{2-} no protonation reactions are included in the database.

3. RESULTS AND DISCUSSION

The following subsections present and compare results of aqueous speciation and solubility calculations obtained from both groups. All calculation results are compiled in tables in the Appendix (Table A.2.1, A.2.2, A.2.3, A.2.4, A.2.5, A.2.6, A.2.7). Explanation for seven RNs behavior in five different cases representative for the LIT is given, starting with those radionuclides not presenting redox reactions in aqueous solution (i.e. Th and Am). Recommendations for building a geochemical conceptual modelling approach to be used in a RN reactive transport model for the LIT are provided. Geochemical calculations that are in need of more experimental evidence regarding RN chemical understanding are also highlighted.

3.1. Thorium (Th) – analog of tetravalent actinides

Thorium was not included in the LIT experiment, but used as a redox stable analog of tetravalent actinides in the thermodynamic calculations to facilitate the interpretation and understanding of the uranium, neptunium and plutonium behavior and mobility in the LIT experiment. Th, as a non-redox sensitive actinide, shows very similar behavior in the studied waters due to the formation of $Th(OH)_4(aq)$ as the predominant aqueous species in all cases (see Table A.2.1). Ternary hydroxo-carbonato complexes, like $Th(CO_3)(OH)_3^-$ are also relevant under the studied conditions, being present at relative abundances between 28-45%, mainly depending on the pH of the water and showing more relevance at higher pH´s. As predicted by Group B, the $Th(OH)_3^+$ species would only account for a few percent of the speciation (< 8%) in the less alkaline bentonite waters (BPW). However, it should keep in mind that thermodynamic data for $Th(OH)_3^+$ was only estimated (Grivé et al. 2010) and that the same complex was not included in the database used by Group A following the argumentation in Rand et al. (2008) and Thoenen et al. (2014). Although the formation of $Th(OH)_3^+$ has been reported in in several studies (Neck et al. 2001, Bentouhami et al. 2004), it is clear that, if present, this would be only as minor species not playing a significant role in the migration of Th or actinides in their tetravalent state (i.e. U, Np or Pu).

Both, modeler groups selected an amorphous $ThO_2(s)$ as the solid that could limit the concentration of Th in aqueous solution to concentrations below < $1x10^{-8}$ M. The maximum concentrations calculated for all the waters are very similar and mainly depend on the crystallinity and particle size of the solid selected. However, the possible existence of tetravalent actinide-bearing colloids, namely “eigencolloids” (particle size between 20 and 300 nm) in the studied waters can not be neglected (Altmaier et al. 2013) which would result in a higher concentration of thorium (or tetravalent actinides) in solution than expected from these calculations.

3.2 Americium (Am)

Am(III) is the only stable oxidation state, making redox conditions irrelevant for the mobility of this RN. In general, there is a good agreement between the aqueous speciation calculations performed by both groups (see Table A.2.2). Silicates were identified to form strong aqueous complexes with Am(III), as $AmOSi(OH)_3^{2+}$, in the near neutral pH of the bentonite (BPW) and mixed (MW) waters. Only in the more alkaline Grimsel groundwater, GGW (pH 9.6) the carbonate complexes and the hydrolysis species are found to be more relevant (see Figure 1).

Main differences in the calculations performed by both groups are related to the different thermodynamic data used for the complex $AmOSi(OH)_3^{2+}$. Although, the silicate complexes of americium and other analog trivalent cations like Eu and Cm in aqueous solution have been proofed by different experimental techniques, e.g. solvent extraction (Jensen and Choppin, 1996, Thakur et al. 2007) or TRLFS (Panak et al. 2005), thermodynamic data derived from these studies reveals contradicting findings, reflected in different thermodynamic data of about 0.6 log units in the databases used by both groups (see Table A.10). Recently, Grenthe et al. (2020) highlighted the complexity of studying Am(III) in silicate-containing waters due to the pH-dependent chemistry of silicates and the formation of colloidal silica species. A value of logβ = -1.71 was selected by Grenthe et al. (2020) for the complex $AmOSi(OH)_3^{2+}$which is in agreement with the value used by Group A (see Table A.10). As revealed by the simulations of both groups, the formation of the Am-silicate complex is expected to play an important role in the studied scenario, however thermodynamic data used by Group B could slightly underestimate the relevance of $AmOSi(OH)_3^{2+}$ in the studied system. In addition, the existence of colloidal "Am(III)−Si" species in the studied waters could be possible (Altmaier et al. 2013), though thermodynamic data are not available and for this reason unpredicted in these calculations. For all the reasons mentioned above, in order to assess the relevance of colloidal "Am(III)-Si" and Am-silicates complexes, further experimental research efforts would be needed to properly predict the behavior of Americium in the LIT experiment.

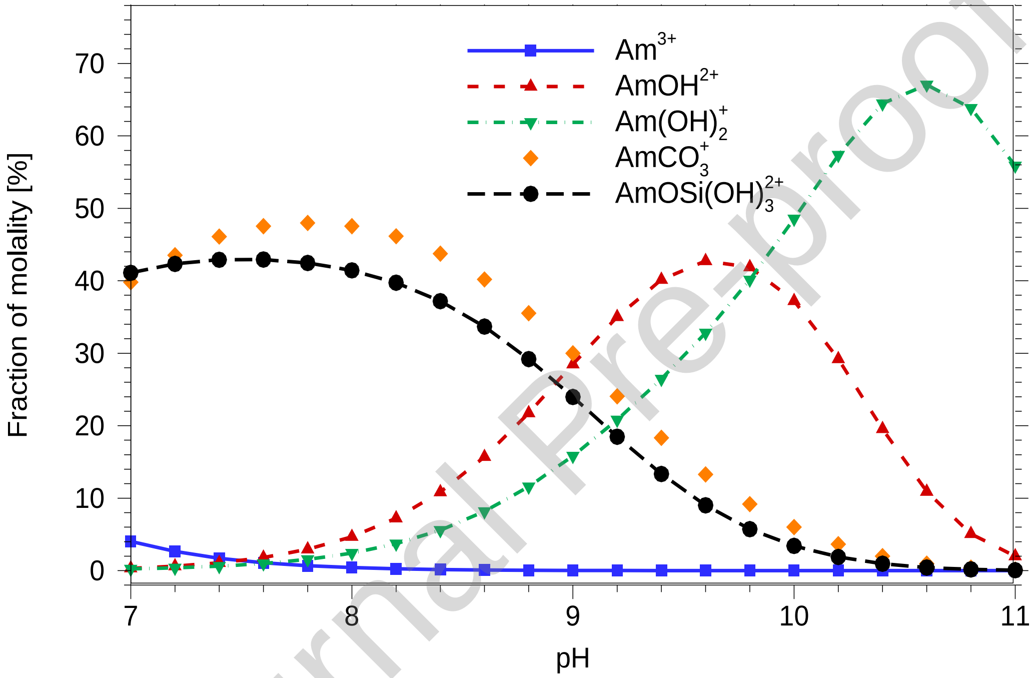

Figure 1 Speciation of Americium as a function of pH considering the GGW composition. Americium concentration = $4x10^{-10}$ mol L^{-1}.

The modeler groups revealed that the solid phases that could precipitate in the different waters were the amorphous mixed hydroxocarbonato complex, $Am(CO_3)(OH)$ (am) in the case of the bentonite (BPW) and mixed (MWO) waters and the amorphous form of the hydroxide, $Am(OH)_3$(am) in the more alkaline system (GGW), highlighting the relevance of the pH and carbonate content of the waters for the precipitation of this radionuclide. The maximum concentrations calculated from Group A is always 1.3 to 2.2 times higher than the Group B which is due to a different stability constant for the $AmOSi(OH)_3^{2+}$ complex in the databases (see explanation above).

As observed in

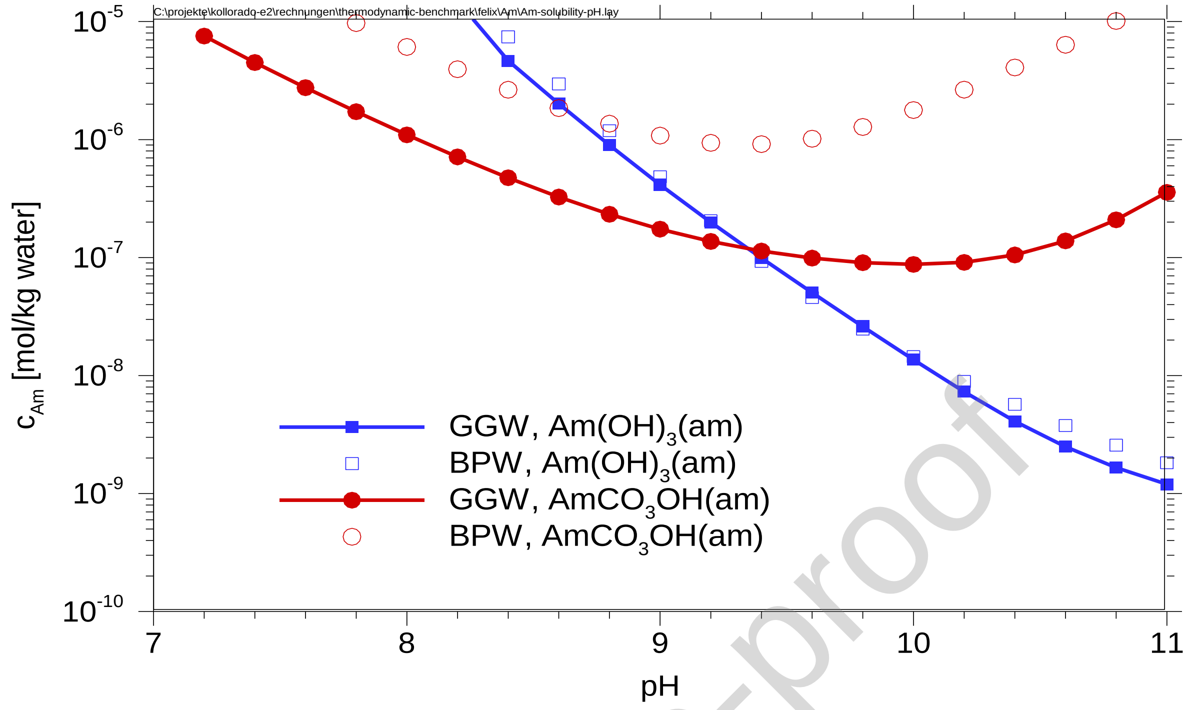

Figure 2 higher concentrations of Am could exist in the bentonite porewater (up to 2 – 4x10^{-5} mol L^{-1}), due to the higher solubility of Am(CO$_3$)(OH) at lower pH´s. At higher pH the calculated concentrations of both groups are 3-6x10^{-7} mol L^{-1} (pH = 9) for the MWs and 5-8x10^{-8} mol L^{-1} for the GGW (pH =9.6), observing lower Am concentrations in the Grimsel groundwater (GGW) due to a change of the solid that could limit the solubility. However, Am was initially included as ^{241}Am with a concentration of 3x10^{-10} mol L^{-1} in the LIT experiment which means that no precipitation of americium would occur in the studied system.

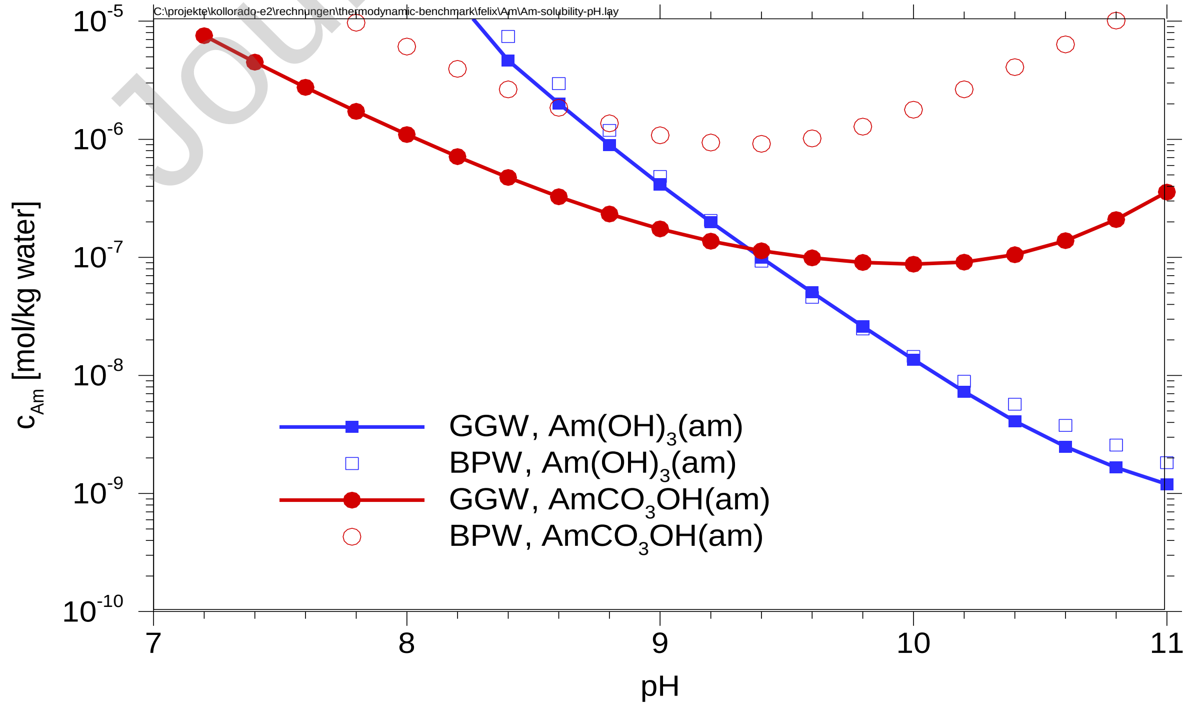

Figure 2 Maximum Am concentration in the bentonite pore water (BPW) and in Grimsel ground water (GGW) calculated for $Am(OH)_3(am)$ and $Am(CO_3)(OH)(am)$ as solubility limiting phase in dependence of pH

3.3. Selenium (Se)

Selenium was initially included with a concentration of $1x10^{-5}$ mol L^{-1} as $^{75}Se(+VI)$ in the LIT experiments. However, due to the reducing conditions of the BPWR, GGW and MWR, Se could be reduced to Se(-II) according to the thermodynamic calculations performed by both groups (see Table A.2.3). However, it should be kept in mind that redox reactions (see Eq. 1) with high electron and proton transfer, including the break of chemical bonds (i.e. Se-O) are energetically expensive (Koper, 2013) and normally kinetically driven with the need of a catalyst (e.g. microbial activity or inorganic surfaces like green rust). Actually, microbial activity in the LIT experiment could be possible (Gillow et al., 2000, Haynes et al., 2021) and promote selenium reduction (Behrends et al. 2012).

$$SeO_4^{2-} + 9\ H^+ + 8e^- \rightarrow\ HSe^- + 4\ H_2O \qquad (1)$$

Depending on the thermodynamic database used, it is predicted that Se is present in the three reducing waters BPWR, MWR, and GGW as HSe^- or as a mixture of HSe^- and polyselenides (Se_3^{2-} and Se_4^{2-}). Although the formation of polyselenides in aqueous solution is well documented, thermodynamic data for these species are still scarce and data for their protonation are not existing (Thoenen et al. 2014). For this reason, polyselenides species and their associated thermodynamic data should be used with caution for predicting selenium migration, as their stability is still not clear and further investigations are needed.

On the other hand, for the bentonite water under oxidizing conditions (BPWO), good agreement was observed in the calculations performed by both modelling groups and Se is present in the aqueous solution as SeO_3^{2-} or $HSeO_3^-$ (see Table A.2.3). In contrast, differences were observed in the calculations performed for the oxidizing mixed water (MWO), which are attributed to the different redox conditions, used by both groups (-148 mV vs 100 mV), obtaining either, Se(-II) or Se(+IV) species, respectively (see Appendix, Table A.1).

Another important aspect of the calculations was to identify which solid phases could precipitate in the system. In this sense, one important parameter is the presence of Fe(II) in the aqueous solution which may cause the precipitation of $FeSe_x(s)$ solid phases (with x =1 or 2) giving very low Se concentration in the aqueous solution. The formation of $FeSe_x(s)$ solid phases has been widely described (Olin et al. 2005, Etteieb et al. 2020) and is expected to control Se solubility in reducing environments where Fe(II) is present. However, according to Charlet et al. (2007), Se(VI) and Se(IV) can also be transformed to Se(0) and other reduced Se species in reducing environments. The redox mechanism is not well known, although it seems that the reaction proceeds via sorption onto Fe oxides, with reductive dissolution of the iron minerals, finishing with the precipitation of Se(0), ferroselite or Se-hosting pyrite. In addition, Charlet et al. (2007) observed important Se reduction for pH <7 and the formation of stable insoluble Se(0) in Fe(II)-clay systems. They suggested that other forms of Fe(II) may lead to the reductive precipitation of Se(0) and highlighted the need to investigate further geochemical parameters to determine the long-term stability of Se. Considering thermodynamic calculations of this work, Se(0) is expected to precipitate and to determine the very low selenium concentration (< $1x10^{-8}$ mol L^{-1}) in the aqueous solution in the studied systems with Eh values > -220 mV, as exemplarily shown in Figure 3. Consequently, Se(0) is used as the solubility determining solid phase in the calculations for bentonite (BPW) and Grimsel groundwater (GGW) by both groups. Although the thermodynamic data are similar for both modelling groups, calculated Se concentrations differ for BPWR and GGW. The reason is the consideration of polyselenides in calculations of Group A leading to a slightly higher selenium concentration in solution in the case of the BPWR, but to a one order of magnitude higher concentration in the more alkaline GGW (pH = 9.6). In BPWO the concentrations of Group A and B are similar, since the Se speciation is dominated by oxidized species and polyselenides do not contribute to speciation in solution.

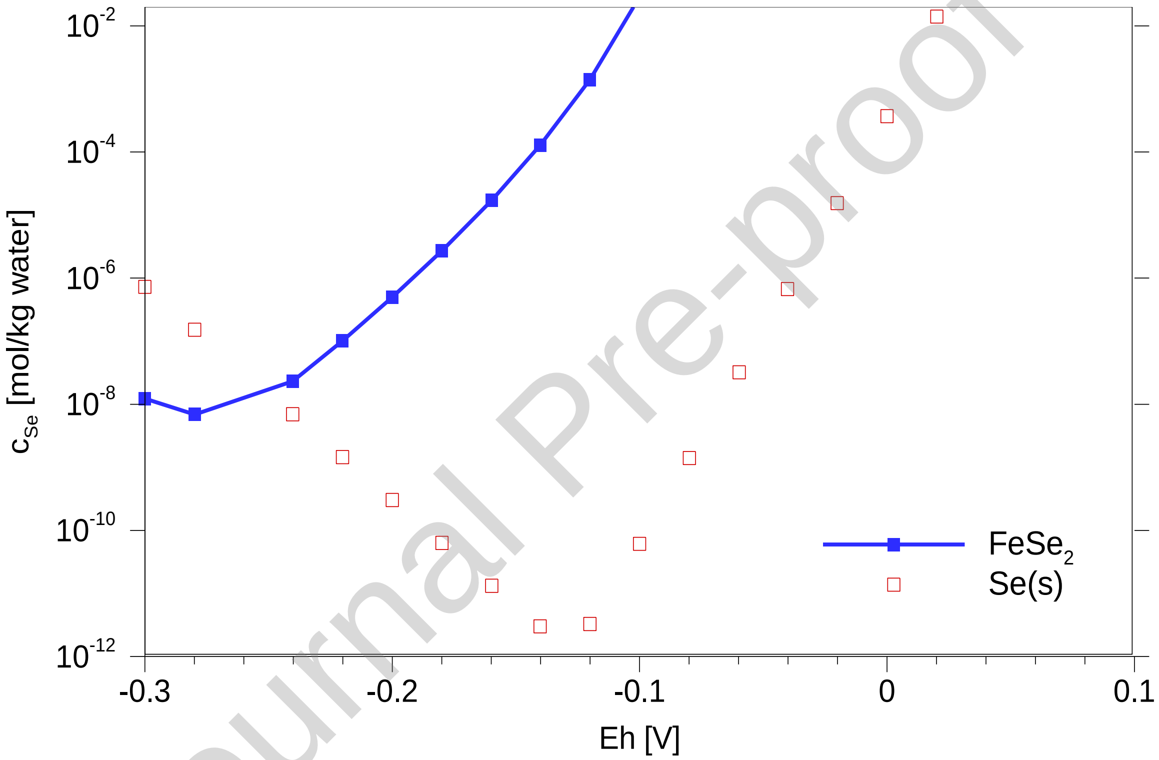

Figure 3 Selenium concentration in the aqueous solution in equilibrium with Se(s) and $FeSe_2$ as function of Eh ([Fe] = $3x10^{-9}$ mol/kg water, pH = 9.6)

The big differences in Se concentration in the MWR and MWO is mainly due to the difference in Eh values and consequently different solid precipitating in the system (i.e. $FeSe_2$, Se(0) or $CaSeO_3 \cdot H_2O$). For the Eh value of -303 mV in MWR Group A selected $FeSe_2$ as solubility determining phase, whereas Group B applied the solid phase Se(0) with Eh = -220 mV (see. Figure 3). The application of both different phases resulted in more than one order of magnitude lower Se concentration determined by Group B. The differences are even more pronounced for MWO, where the Eh-value of +100 mV of Group B results in a speciation dominated by selenite species including $CaSeO_3 \cdot H_2O$ as solubility limiting solid phase. In Group A calculations (Eh = -148 mV), $FeSe_2$ is selected as solid phase precipitating and solution speciation is dominated by polyselenides.

These observations and the general disagreement observed between calculations performed by both groups, clearly indicates that possible formation of polyselenides in these environments should be clarified, specially giving experimental evidences and providing thermodynamic data which are missing. In addition, the redox state of selenium would be needed to be determined experimentally, e.g. by high energy resolution fluorescence detected X-ray absorption spectroscopy (HERFD-XAS) (Bissardon et al. 2019).

3.4. Technetium (Tc)

Technetium was initially included in the experiments with a concentration of 2.4x10^{-5} mol L^{-1} as $^{99}TcO_4^-$. As in the case of Se, technetium is a redox sensitive element, with the most stable redox states being Tc(+IV) and Tc(+VII) under reducing and oxidizing conditions, respectively. Calculations performed by both groups are in good agreement (see Table A.2.4), since the original source of thermodynamic data for the relevant technetium species for both databases is the same (Rard et al. (1999). Differences in the calculations are only attributed to the different redox conditions defined by the mixed waters (MWs), highlighting the relevance of a good experimental definition of the redox conditions of the system.

Tc aqueous speciation is dominated by the hydroxo complex $TcO(OH)_2$ in the BPWR, and GGW. The complex $TcO(OH)_3^-$ only contributes to a few percent in the more alkaline GGW. For the oxidizing BPWO, TcO_4^- is the only relevant species in solution.

The only solid phase that could precipitate in the system is the hydrated oxide TcO_2 x H_2O (x = 1.6 or 1.63) giving very low concentrations of Tc in solution around 4x10^{-9} mol L^{-1} in the BPWR, MWR, GGW. Under oxidizing conditions, no precipitation of Tc will be expected. Due to the low concentration of this RN in the aqueous reducing system, analytic techniques with highly sensitive detection limits is very much advised (Quinto et al. 2017, 2019). In recent literature, new thermodynamic data for $TcO_2{\cdot}0.6H_2O(s)$ was published (Yalcintas, 2016). This new thermodynamic data for $TcO_2{\cdot}0.6H_2O(s)$ is very similar to the one selected in the thermodynamic databases used for this exercise (see Table A.3.4) and within the uncertainty range not showing significant differences in calculations performed with this solid.

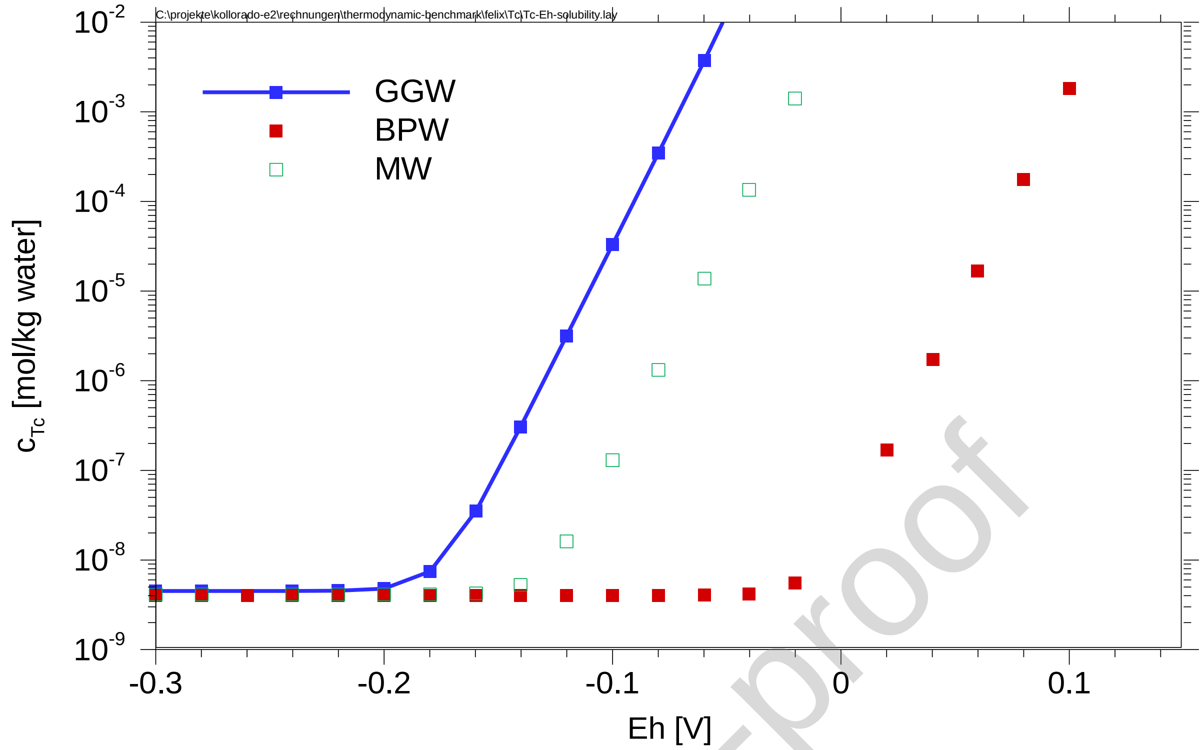

Figure 4: Concentration of Tc in equilibrium with $TcO_2 \cdot x\ H_2O$ (x = 1.6 or 1.63) calculated for GGW (pH = 9.6), BPW (pH =7.4) and MW (pH = 9.0) as function of Eh

3.5 Uranium (U)

Uranium was initially included in the experiments with a concentration of 2.4×10^{-6} mol L^{-1} as $^{233}U(VI)$. The chemistry of uranium is very complex and its speciation in aqueous solutions is continuously studied and updated in databases. Speciation is strongly impacted by the pH and Eh value, the concentration of calcium and carbonate.

Calculations performed by both groups revealed that ternary calcium-uranyl-carbonate complexes dominate the aqueous speciation in all waters. However, the predominance of the complex $Ca_2UO_2(CO)_3(aq)$ and $CaUO_2(CO_3)_3^{2-}$ was very different when comparing the calculations of both groups. These discrepancies were attributed to the difference of 1.5 log units of the thermodynamic data selected for the $Ca_2UO_2(CO)_3(aq)$ complex. Looking in detail to the origin of the thermodynamic data used by Group A, revealed that in fact it was a typo in the data selected for $Ca_2UO_2(CO)_3(aq)$ and not corrected in the original report describing it, as indicated by the own authors (Thoenen et al. 2014). The logβ should be actually 29.8 ± 0.7 (Kalmykow et al. 2000) instead of 29.22 ± 0.25. In addition, should be noted that thermodynamic data used by Group B presents a very huge uncertainty (logβ = 30.7 ± 1.6) which seems to be overestimated considering the recent review of Grenthe et al. (2020). The stability constant selected by Grenthe et al. (2020) for the same complex (logβ = 30.8 ± 0.4), considers much more recent and accurate studies (Endrizzi and Rao, 2014) that the ones used in the databases of Group B.

Therefore, Group A decided to use a logβ = 30.6 ± 0.09 as recommended in the THEREDA database (Richter et al. 2015) instead of 29.22 in their calculations. Note however that the error provided in THEREDA is incorrect and a value of ±0.9 should be used instead considering propagation of uncertainties in statistics (see Appendix C in Grenthe et al. 2020). Applying the new log*β* value for the $Ca_2UO_2(CO)_3(aq)$ complex the speciation of all five waters is much more similar between Group A and Group B and by more than 80% dominated by ternary Ca-uranyl-carbonate complexes. The complex $Ca_2UO_2(CO)_3(aq)$ was always prevailing in solution as predominant and only under the more alkaline conditions of the GGW, the $CaUO_2(CO_3)_3^{2-}$ complex was more stable. Interestingly, calculations indicated that the redox conditions of the studied system are not relevant for uranium, although being a redox sensitive element, and uranium will be mainly present as U(VI) in the aqueous solution due to the high stability of ternary complexes Ca–U(VI)–carbonate (Figure 6). Only in BPWR and MWR tetravalent uranium occurred to few percent in the form of $U(OH)_4$ or $UCO_3(OH)_3^-$, the former only appearing in the calculations of Group A. It appears that very little experimental data on ternary U(IV) hydroxide carbonate species is available which is underpinned by the fact that $UCO_3(OH)_3^-$ is not considered in the database of Group B. Scoping calculations by Hummel et al. (2002) showed that $UCO_3(OH)_3^-$ can have some relevance in environmental modeling although it is clear that this complex will not play any role in the studied system.

Contrarily to the aqueous speciation, the maximum uranium concentration in the aqueous solution and the solubility determining phase are strongly affected by the pH and Eh values. As exemplarily shown in Figure 5 for GGW and MW amorphous, hydrated UO_2 (am) determines the solubility under reducing conditions and lower pH´s (BPWR) whereas uranophane is considered relevant in the Eh range above -300 mV and pH > 9. Calculated concentrations of both modeler groups are rather similar (using the corrected logß value for the Ca-U-carbonate) and always higher than the initial uranium concentration included in the system, this means that no precipitation of uranium would be expected in the LIT experiments. Although a priori, these observations could indicate that the thermodynamic data for uranium are well established, the diversity of uranyl minerals that possibly form in the presence of Ca-Mg-Na-K-Si-carbonate-SO_4-Cl in the near neutral –moderately alkaline conditions and their corresponding thermodynamic data (Nguyen et al. 1992, Shareva et al. 2011, Richter et al. 2015) have not been fully explored with respect to understanding potential mineral transformations (Stanley and Wilkin, 2019) and would be strongly advised.

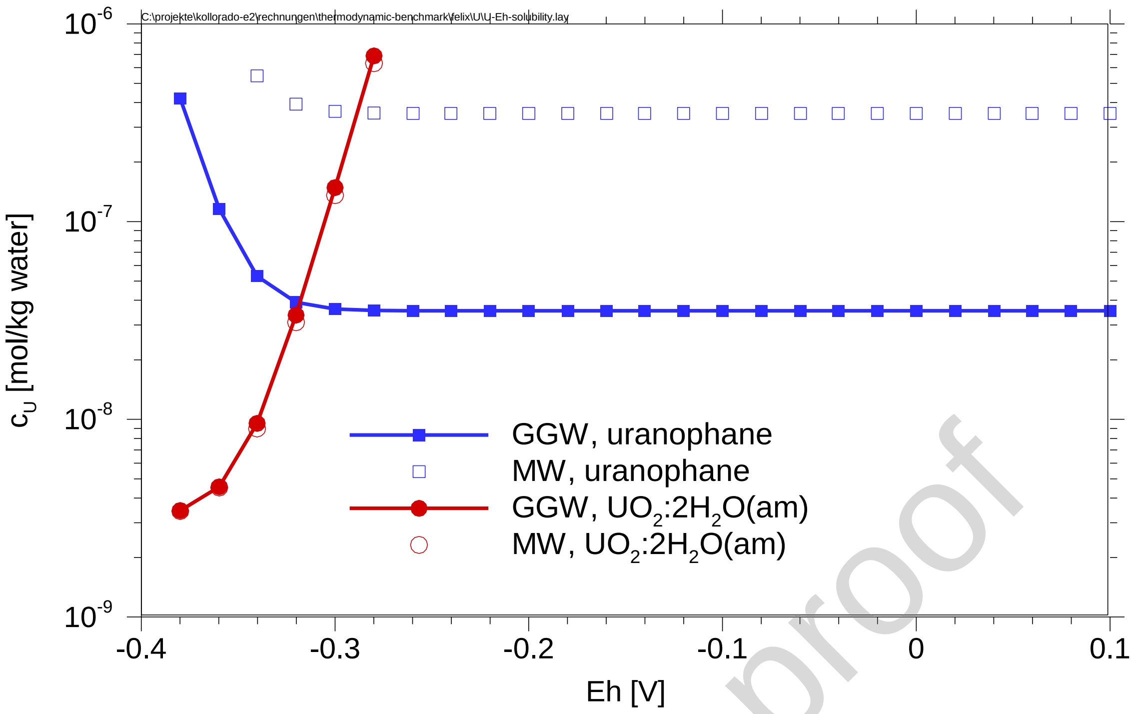

Figure 5 Solubility of uranium in equilibrium with $UO_2 \cdot 2H_2O$(am) and uranophane for GGW (pH = 9.6) and MW (pH = 9) as function of Eh

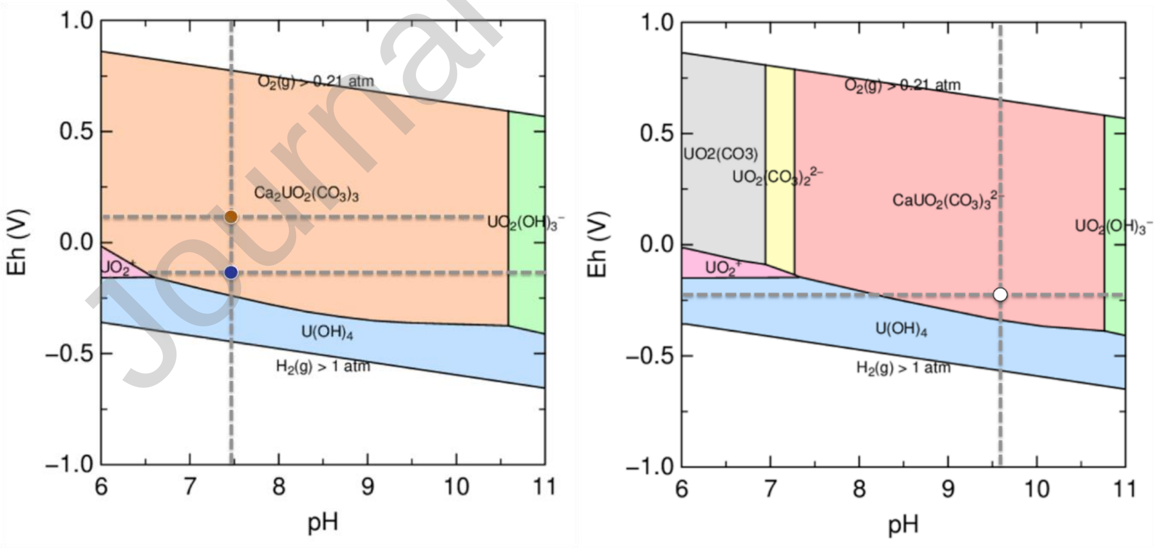

Figure 6 Pourbaix diagram of uranium (c= $4x10^{-10}$ mol L^{-1}) in BPW (left) and in GGW (right). The red dots show the pH/Eh conditions of BPWR, BPWO and GGW.

3.6 Neptunium (Np)

Neptunium was initially included as ^{237}Np(V) with a concentration of $5.0x10^{-5}$ mol L^{-1} in the LIT experiment. Neptunium presents different oxidation states from +III to +VI depending on the redox conditions, although Np(+IV) was the most stable redox state for the reducing waters (BPWR, MRW) and GGW, with $Np(OH)_4$ (aq) as predominant aqueous species. Only in BPWO and MWO with highest Eh values, also Np(V) aqueous species were present. In fact, only Group B predicted the formation of Np(V) aqueous species in MWO due to the higher Eh used. On the other hand, big discrepancies exist between calculations performed by Group A and B with the BPWO, due to the inclusion or exclusion of the Np(V)-silicate complex in their respective databases. The stability constant of $NpO_2SiO(OH)_3$ (see Table A.14) is only included in the database used by Group A which was determined by Pathak and Choppin (2007) by solvent extraction methods. This value is very high ($\log\beta = 7.0$) compared to both, the one reported by Yusov et al. (2005) obtained by spectroscopic methods ($\log\beta = 2.3$) at ionic strength of 0.1 mol L^{-1} and to stability constants for analogous silicate complexes (Thoenen et al., 2014). Recently, Grenthle et al. (2020) also criticized the extremely high value reported by Pathak and Choppin (2007), indicating that the value $\log\beta = 7.0$ is inconsistent with the estimated values obtained by the linear free energy relationship between hydroxides and silicates species proposed by Jensen, (1994). Considering these conflicting evidences about the complexation strength of Np(V) silicate, it seems that the calculation performed by Group A are probably over predicting the relevance of silicate complexes in the bentonite water at oxidizing conditions (BPWO). In fact when a value of logβ between 2.3 and 5.3 is used in the calculations of Group A, the predominant aqueous speciation between both groups is very similar, indicating that although the complex $NpO_2SiO(OH)_3$ could exist in aqueous solution, its high stability and predominance in BPWO is doubtful (Shilov et al. 2004).

Aqueous Np concentrations under the conditions of interest are expected to be controlled by the precipitation of neptunium (IV) dioxide, giving concentrations < $7x10^{-9}$mol L^{-1}. No important differences are observed in the solubility calculations for all reducing waters when using the different databases, which is due to the fact that the controlling aqueous species is the neutral $Np(OH)_4$(aq) in most cases. Hence, there are no important activity corrections and the thermodynamic data for $Np(OH)_4$(aq) and for the solid neptunium (IV) dioxide are similar.

Differences in calculated neptunium concentrations only occur in the more oxidizing waters BPWO and MWO, where Np(V) species are relevant. Concentrations more than three times higher in BPWO were derived by Group A and result from the contribution of the strong $NpO_2SiO(OH)_3$ complex, which is not considered by Group B and it is probably overestimated by Group A as indicated above. In case of MWO the higher concentration calculated by Group B is caused by the high Eh value of 100 mV and the corresponding predominance of Np(V) species, whereas in case of Group A for an Eh value of -148 mV $Np(OH)_4$(aq) is the relevant species in solution.

3.7 Plutonium (Pu)

Plutonium was initially included as ^{242}Pu(IV) with a concentration of $8.6x10^{-9}$ mol L^{-1} in the LIT experiment. Pu presents different redox states (+III, +IV, +V and +VI) in solution, although according to the thermodynamic simulations, Pu is mainly present in the oxidation states (+III) and (+IV) during the evolving conditions of the LIT experiment (see Table

A.2.7). The formation of Pu aqueous species (and solid phases) depends mainly on the Eh and pH of the system. The presence of carbonates and/or sulphates, specially under near neutral reducing conditions, could also play a role in the aqueous complexation of Pu in solution (i.e. BPWR). The significance of silicates on Pu in the studied system is critical and unknown. Although silicates are abundant in the studied waters (> 10^{-4} M) there are very few experimental data reporting the interaction of redox sensitive actinides, like Pu, with silicate. Main reason for the lack of this information is the complexity of actinide-silicate systems, including multiple parallel processes, such as the pH- and time-dependent 16olymerization of silicic acid, the competing hydrolysis reactions of the actinides, and especially the formation of Pu(IV) colloids (Grenthe et al. 2020). This complexity is reflected in the discrepancies observed between the calculations performed by Group A and B with the BPWR, due to the inclusion or exclusion of the Pu(III)-silicate complex in their respective databases. Thermodynamic data for $PuSiO(OH)_3^{2+}$ was only estimated base on analogies with Am(III), Eu(III) and Cm(III) in the database used by group A (Thoenen et al. (2014), although the formation of this complex has never been proved experimentally. The same complex was not included in the database used by group B. As a consequence, $PuSiO(OH)_3^{2+}$ is the dominating species obtained by Group A for the BPWR, whereas the Pu(III) carbonates, sulphates and hydrolyzed Pu(III) dominate the aqueous Pu speciation in the calculations from Group B. At the present moment, the lack of experimental data on Pu(III) silicate complex formation and the uncertainty of the data on chemical analogues with $AmOSi(OH)_3^{2+}$ (see section 3.2) complicates the evaluation of the accuracy of the estimated data used by Group A. These clearly indicates that possible formation of Pu(III)-silicates in bentonite barriers at reducing conditions should be clarified giving experimental evidences and providing accurate thermodynamic data in the future.

Due to the higher pH and Eh of the GGW, MWs and BPWO, Pu(IV) dominates the aqueous speciation of these waters. However, considerable differences are observed in the calculations depending on the thermodynamic database used. Under the conditions of the studied systems this concerns particularly to the formation of $Pu(OH)_4$ and $Pu(CO_3)(OH)_3^-$. In calculations of Group B, $Pu(OH)_4$ is predominant, whereas in the Group A calculations the contribution of $Pu(CO_3)(OH)_3^-$ is more than 90 %. Even though there are no reliable experimental data on the formation of ternary Pu(IV) hydroxide-carbonate complexes as discussed in Grenthe et al. (2020), thermodynamic data for $Pu(CO_3)(OH)_3^-$ has been estimated in Hummel and Berner, (2002) using a “backdoor approach” and included in the database used by Group A, where this species is not considered in the database used by Group B.

All these differences and discrepancies in the calculations, highlight the need of study further the aqueous speciation of Pu in presence of both, carbonate and silicates and to derive appropriated and consistent thermodynamic data which is still lacking.

Both, Group A and B considered the solid PuO_2(am) in all systems as the solubility limiting phase. However, in all calculations of Group B the maximum concentration was higher. The main reason for this difference is the large difference in solubility products used by Group A (logK = -2.33 ± 0.52) and by Group B (logK = -0.80 ± 1.30) for PuO_2(am). The data used from Group A originates from the review of Guillaumont et al. (2003) and it is discussed in Thoenen et al. (2014) where it is described that this solubility product only applies to precipitated solids that were aged for several months near room temperature, freshly precipitated solids may be more soluble. However looking to the uncertainty of the stability constant used by Group B, it is clear there is more than 1 order of magnitude of difference in the concentration expected for Pu in the studied system.

4 CONCLUSIONS

The benchmark exercise of the speciation and solubility calculations of seven radionuclides under the geochemical boundary conditions of the Long- in situ Test (LIT) in Grimsel, Switzerland has shown that the geochemical parameters (i.e. pH, redox, carbonate, silicate, iron and calcium concentrations) should be clearly monitored in order to have a good prediction of radionuclide migration in a bentonite barrier included in a nuclear waste repository concept in crystalline rock. Radionuclide speciation and evolution is expected to be completely different from one radionuclide to another. In general, very low concentrations of all the studied radionuclides (i.e. ^{75}Se(VI), ^{99}Tc(VII),^{233}U(VI), ^{237}Np(V), ^{241}Am(III), Th(IV) and ^{242}Pu(IV)) is expected which limit the number of available experimental techniques, with low detection limits, able to determine their chemical speciation. This highlith the importance of determining the chemical speciation by thermodynamic calculations, specially, in terms of confidence, robustness and tracability of the thermodynamic data (stability constants) used.

The findings of the current investigate, indicate that differences in the aqueous speciation and solubility calculations by using different state of the art thermodynamic databases for the non-redox sensitive radionuclides, Thorium and ^{241}Am(III) are minimum and within the uncertainty range of the thermodynamic data. From one side, the geochemical evolution of the LIT, specially the pH and carbonate concentration, have minimum effects in thorium chemistry and major uncertainties arises from inclusion/exclusion of tetravalent actinide-bearing colloids. From the other side Am-silicate complex is expected to play an important role in the studied scenario where thermodynamic data present high uncertantines and should be carefully studied in the future. In addition, the existence of colloidal “Am(III)−Si” is possible, though, thermodynamic data is not available and for this reason unpredicted in these calculations.

Differences of the chemical behavior for the redox sensitive radionuclides greatly depend on the specific radionuclide considered. From one side, calculations with Tc performed by both groups are in good agreement and differences in the calculations are only attributed to the different redox evolution of the system, highlighting the relevance of a good experimental definition and measurement of the redox conditions. On the other hand, Se chemistry is also greatly influence by the redox evolution of the system but also by the formation of polyselenides which, thermodynamic data are still scarce and data for their protonation are not existing. Calculations performed by both groups for uranium revealed that ternary calcium-uranyl-carbonate complexes dominate the aqueous speciation in all waters, highlighting the high stability of these complexes even at reducing conditions. Comparison also allowed to correct thermodynamic data for one of the databases which was incorrectly introduced and documented. Contrarily to the aqueous speciation, the maximum uranium concentration in the aqueous solution and the solubility determining phase are strongly affected by the pH and Eh. Finally, discrepancies obtained in the calculations performed for Np and Pu are mainly due to the consideration or not of Np(V)-silicates or Pu(III)- silicate complexes which thermodynamic data present high uncertainties due to the difficulty of studying these systems (i.e. time-dependent polymerisation of silicic acid, competing hydrolysis reactions of the actinides, and the formation of Actinides(IV) eigencolloids). In the specific case of Np, silicates are only relevant under oxidizing conditions and present thermodynamic data is highly unreliable and Pu(III)-silicate formation have never been proved experimentally.

As demostrated, benchmarking thermodynamic calculations to determine radionuclide speciation under realistic and representative conditions, helps to identify gaps in data and concepts and bring confidence in long-term predictions.

Acknowledgement

This work was financed by the German Federal Ministry of Economic affairs and Energy (BMWi) under Contract nos 02 E 11456A and 02 E 11456B. We also would like to thank the partners from the CFM project at Grimsel Test Site NAGRA (Switzerland), JAEA and NUMO (Japan), POSIVA (Finland), DOE (USA), KAERI (South Korea), RWM (UK) and CIEMAT (Spain). Additionally, V. Montoya acknowledge the German Federal Ministry of Education and Research (Grant 02NUK053A) and the Initiative and Networking Fund of the Helmholtz Association (Grant SO-093) within the iCross project for partial funding.

References

Alonso, U., Missana, T.; Geckeis, H.; García-Gutiérrez, M.; Turrero, M.J.; Möri, R.; Schäfer, Th.; Patelli, A.; Rigato, V. 2006. Role of inorganic colloids generated in a high-level deep geological repository in the migration of radionuclides: Open questions. Journal of Iberian Geology, 32, 79-94

Altmaier, M.,Gaona, X. Fanghänel, T., 2013. Recent Advances in Aqueous Actinide Chemistry and Thermodynamics. Chemical Reviews, 113, 901-943

Baik, M-H; Lee, S-Y; Lee, J-K; Kim, S-S; Park, C-K; Choi, J-W., 2008. Review and compilation of data on radionuclide migration and retardation for the performance assessment of a HLW repository in Korea. Nuclear Engineering and Technology, 40, 593

Behrends, T., Krawczyk-Bärsch, E., Arnold, T. 2012. Implementation of microbial processes in the performance assessment of spent nuclear fuel repositories. Applied Geochemistry, 27, 453

Bennett, D.G., 2014. Radionuclide Solubility Limits in SKB´s Safety Case. Main Review Phase. Report Number 2014:11. Swedish Radiation Safety Authority (SSM), Sweden.

Bentouhami, E., Bouet, G. M., Meullemeestre, J., Vierling, F., Khan, M. A., 2004. Physicochemical study of the hydrolysis of rare-earth elements(III) and thorium(IV), Compt. Rend. Chimie, 7, 537545.

Bissardon, C., Proux, O., Bureau, S., Suess, E., Winkel, L.H.E., Conlan, R.S., Francis, L.W., Khan, I.M., Charlet, L., Hazemann, J.L., Bohic, S., 2019. Sub-ppm level high energy resolution fluorescence detected X-ray absorption spectroscopy of selenium in articular cartilage. Analyst, 144, 3488-3493.

Bruno, J., Duro, L., Rollin, C., Guimera, J. (eds.), 2000. Prediction of the solubility and speciation of RN in Febex and Grimsel waters. Version 1.1. QuantiSci report, Barcelona.

Charlet L., Scheinost, A.C., Tournassat C., Grenechee G.M, Géhina A., Fernández-Martínez M., Coudert S., Tisserand T., Brendleg, J., 2007. Electron transfer at the mineral/water interface: Selenium reduction by ferrous iron sorbed on clay, Geochimica et Cosmochimica Acta, 71, 5731-5749

Dong, W. M., Brooks, S. C., 2006. Determination of the formation constants of ternary complexes of uranyl and carbonate with alkaline earth metals (Mg^{2+}, Ca^{2+}, Sr^{2+}, and Ba^{2+}) using anion exchange method. Environ. Sci. Technol., 40, 4689.

Duro, L., Grivé, M., Cera, E., Gaona, X., Domènech, C., Bruno, J., 2006. Determination and assessment of the concentration limits to be used in SR-Can. Technical Report TR-06-32.

Duro, L.; Montoya, V., Colàs E., García, D. 2010. Groundwater equilibration and radionuclide solubility calculations. Technical report NWMO TR-2010-02, Canada

Endrizzi, F., Rao, L., Chemical speciation of uranium(VI) in marine environments: complexation of calcium and magnesium ions with $[(UO_2)(CO_3)_3]^{4-}]$ and the effect on the extraction of uranium from seawater, Chem. Eur. J., 20, 14499

Etteieb, S., Magdouli, S., Zolfaghari M, Kaur Brar S., 2020. Monitoring and analysis of selenium as an emerging contaminant in mining industry: A critical review. Science of the Total Environment, 698, 134339

Fernandez, A.M., Baeyens, B., Bradbury, B., Rivas, P., 2004. Analysis of the porewater chemical composition of a Spanish compacted bentonite used in an engineered barrier. Phys. Chem. Earth 29, 105–118.

Giffaut, E., Grivé, M., Blanc, Ph., Vieillard, Ph., Colàs, E., Gailhanou, H., Gaboreau, S., Marty, N., Madé, B., Duro, L., 2014. Andra thermodynamic database for performance assessment: ThermoChimie. Applied Geochemistry 49, 225-236.

Gillow, J.B., Dunn, N. Francis, A.J., Lucero D.A., Papenguth. H.W, 2000. The potential of subterranean microbes in facilitating actinide migration at the Grimsel Test Site and Waste Isolation Pilot Plant. Radiochimica Acta, 88, 769

Grenthe, I, Gaona, X, Plyasunov, A, Rao, L, Runde, W, Grambow, B, Konigs, R, Smith, A, Moore, E., 2020. Second Update of the Chemical Thermodynamics of Uranium, Neptunium, Plutonium, Americium and Technetium OECD NEA.

Grivé, M.; Domènech, C.; Montoya, V.; Garcia, D.; Duro, L. 2010a. Simple Functions Spreadsheet tool presentation, SKB TR-10-61 report, Sweden.

Grivé, M.; Domènech, C.; Montoya, V.; Garcia, D.; Duro, L. 2010b. Determination and assessment of the concentration limits to be used in SR-Can. Supplement to TR-06-32, SKB TR-10-50 report, Sweden.

Grivé, M.; Montoya, V.; Duro, L. 2008. Assessment of the Concentration Limits for Radionuclides for Posiva. Working report 2007-103, Finland.

Grivé, M., Riba, O., Montoya, V., Duro, L. 2010. Update of a thermochimie database: Reporting of new data selection 2010. Project ANDRA-TDB6-Task 1, 1st PR Amphos 21.

Guillaumont, R., Fanghänel, T., Fuger, J., Grenthe, I., Neck, V., Palmer, D. A., Rand, M. H., 2003. Chemical Thermodynamics Vol. 5. Update on the chemical thermodynamics of uranium, neptunium, plutonium, americium and technetium. OECD/NEA, Elsevier, Amsterdam.

Harrison, J.J, Payne T.E, Wilsher, K.L., Thiruvoth, S., Child, D.P., Johansen, M.P., Hotchkis, M.A.C. (2016). Measurement of ^{233}U/^{234}U ratios in contaminated groundwater using alpha spectrometry. Journal of Environmental Radioactivity, 151, 537

Hoyer, E-M, Luijendijk, E., Müller, P., Kreye, P., Panitz, F., Gawletta, D., Rühaak, W., 2021 Preliminary safety analyses in the high-level radioactive waste site selection procedure in Germany. Adv. Geosci., 56, 67–75

Haynes, H.M., Bailey, M.T., Lloyd, J.R. 2021 Bentonite barrier materials and the control of microbial processes: Safety case implications for the geological disposal of radioactive waste. Chemical Geology, 581, 20 120353

Hummel, W., Berner, U., 2002. Application of the Nagra/PSI TDB 01/01: Solubility of Th, U, Np and Pu. Nagra Technical Report NTB 02-12, Nagra, Wettingen, Switzerland

Hummel, W., Berner, U., Curti, E., Pearson, F.J., Thoenen, T., 2002. Nagra/PSI Chemical Thermodynamic Data Base 01/01. Nagra NTB 02-16, Nagra, Wettingen, Switzerland.

Jensen, M. P., 1994. Competitive complexation studies of europium(III) and uranium(VI) complexation by aqueous orthosilicic acid, Ph. D. Thesis.

Jensen, M.P. & Choppin, G.R., 1996. Complexation of Europium(III) by Aqueous Orthosilicic Acid. Radiochim. Acta, 72, 143–150.

Kalmykow, S.N. and Choppin, G.R., 2000. Mixed $Ca^{2+}/UO_2{}^{2+}/CO_3{}^{2-}$ complex formation at different ionic strengths. Radiochimica Acta, 88, 603–606.

Kelly, M.J., Hunter, F.M.I. and Swanton, S.W., 2012. Treatment of colloids in post-closure safety assessment, Serco Report SERCO/TAS/002924/02 Issue 02.

Kinniburgh, D. and Cooper, D., 2011. PhreePlot – Creating graphical output with PHREEQC User Manual. 616 p.

1.1 Kolomá. K., Červinka, R., Hanusová, I. 2018. 137Cs transport in crushed granitic rock: The effect of bentonite colloids. Applied Geochemistry, 96, 55-61

Koper, M.T.M., 2013. Theory of multiple proton–electron transfer reactions and its implications for electrocatalysis Chemical Sciences, 7, 2710-2723.

Kurosawa, S., Ueta, S. 2001. Effect of colloids on radionuclide migration for performance assessment of HLW disposal in Japan. Pure Appl. Chem., 73, 2027

Lee, J.-Y., Amayri, S., Montoya, V., Fellhauer, D., Gaona, X., Altmaier, M., 2019. Solubility and stability of liebigite, $Ca_2UO_2(CO_3)_3 \cdot 10H_2O(cr)$, in dilute to concentrated NaCl and $NaClO_4$ solutions at T = 22–80 °C. Applied Geochemistry, 111, 104374

Lemire, R., Taylor, P., Palmer, D., Schlenz, H., 2020. Chemical thermodynamics of iron. Part 2. OECD NEA.

Moog, H.C., Bok, F., Marquardt, C.M., Brendler, V., 2015. Disposal of Nuclear Waste in Host Rock formations featuring high-saline solutions – Implementation of a Thermodynamic Reference Database (THEREDA). Appl. Geochem. 55, 72-84. http://dx.doi.org/10.1016/j.apgeochem.2014.12.016.

Neck, V., Kim, J. I., 2001. Solubility and hydrolysis of tetravalent actinides, Radiochim. Acta, 89, 1-16.

Nguyen, S. N., Silva, R. J., Weed, H. C., Andrews J. E., 1992. Standard Gibbs free energies of formation at the temperature 303.15 K of four uranyl silicates: soddyite, uranophane, sodium boltwoodite, and sodium weeksite, J. Chem. Thermodynamics 24, 359–376.

Novikov, A.; Kalmykov, S.; Utsunomiya, S.; Ewing, R.C; Horreard, F.; Merkulov, A; Clark, S.B; Tkachev, V.V.; Myasoedov, B.F. 2006. Colloid Transport of Plutonium in the Far-Field of the Mayak Production Association, Russia. Science, 314, 638

Nykyri M., Nordman H., Marcos N., Löfman J., Poteri A., Hautojärvi A. Radionuclide Release and Transport – RNT-2008, Posiva Report 2008-06, Posiva Oy, Eurajoki. 2008.

Olin O.A., Nolang, B., Osadchii, E. G., Ohman, L. O., Rosen, E., 2005. Chemical thermodynamics Vol. 7: Chemical thermodynamics of selenium, Elsevier, NEA.

Panak, P.J., Kim, M.A., Klenze, R., Kim, J.I., Fanghänel. Th., 2005. Complexation of Cm(III) with aqueous silicic acid. Radiochim. Acta, 93, 133–139.

Parkhurst, D. L. and Appelo, C., 2013. Description of input and examples for PHREEQC version 3: A computer program for speciation, batch-reaction, one-dimensional transport, and inverse geochemical calculations. In U.S. Geological Survey Techniques and Methods, book 6, volume A43 of Modeling Techniques. U.S. Geological Survey, Denver, Colorado.

Pathak, P.N. and Choppin, G.R., 2007. Silicate complexation of NpO_2^+ ion in perchlorate media. J. Radioanal. Nucl. Chem. 274, 3–7.

Quinto, F., Blechschmidt, I., Garcia Perez, C., Geckeis, H., Geyer, F., Golser, R., Huber, F., Lagos, M., Lanyon, B., Plaschke, M., Steier, P., Schäfer, T., 2017. Multiactinide Analysis with Accelerator Mass Spectrometry for Ultratrace Determination in Small Samples: Application to an in Situ Radionuclide Tracer Test within the Colloid Formation and Migration Experiment at the Grimsel Test Site (Switzerland). Anal. Chem. 89, 7182–7189.

Quinto, F., Busser, C., Faestermann, T., Hain, K., Koll, D., Korschinek, G., Kraft, S., Ludwig, P., Plaschke, M., Schäfer, T., Geckeis, H., 2019. Ultratrace Determination of ^{99}Tc in Small Natural Water Samples by Accelerator Mass Spectrometry with the Gas-Filled Analyzing Magnet System. *Anal. Chem*., 91, 4585-4591

Rand, M. H., Fuger, J., Grenthe, I., Neck, V., Rai, D., 2008. Chemical Thermodynamics Vol. 11. Chemical Thermodynamics of Thorium. OECD NEA, Paris.

Rard, J.A., Sandino, M.C.A., Östhols, E., 1999. Chemical Thermodynamics of Technetium, OECD NEA

Reiller, P., Descostes, M., 2020. Development and application of the thermodynamic database PRODATA dedicated to the monitoring of mining activities from exploration to remediation. Chemosphere, 251, 126301

Reiller, P.E, Vercouter, T., Duro L., Ekberg, C., 2012. Thermodynamic data provided through the FUNMIG project: Analyses and prospective. Applied Geochemistry, 27, 414-426

Richter, A., Bok, F., Brendler, V., 2015. Data compilation and evaluation for U(IV) and U(VI) for the thermodynamic reference database THEREDA. Wissenschaftlich-Technische Berichte HZDR-065, Helmholtz-Zentrum Dresden-Rossendorf, ISSN 2191-8708.

Rinderknecht, F., Noseck, U., Schäfer, F. (eds.), 2019. Integrity of the bentonite barrier for retention of radionuclides in crystalline host rock – experiments and modeling. KOLLORADO-e^2 Final report. KIT Open Report 7757, Karlsruhe

Sellin, P., Leupin O.X. 2013. The use of clay as an engineered barrier in radioactive-waste management–a review. Clays and Clay Minerals, 61, 477

Schäfer, T., Huber, F., Seher, H., Missana, T., Alonso, U., Kumke, M., Eidner, S., Claret, F., Enzmann, F., 2012. Nanoparticles and their influence on radionuclide mobility in deep geological formations. *Appl. Geochem*. 27, 390-403.

Schlickenrieder, L., Lanyon, G. W., Kontar, K., Blechschmidt, I., 2017. Colloid Formation and Migration Project: Site instrumentation and initiation of the long-term in-situ test; Grimsel Test Site Investigation Phase VI. *NAGRA Technical report*, NTB 15-03.

Shelton, A., Sellin, P., Missana, T., Schäfer, T., Červinka, R., Koskinen, K., 2018. *SKB Technical report* TR-17-17.

Shilov, V. P., Fedoseev, A. M., Yusov, A. B., Delegard, C. H., 2004. Behavior of Np(VII, VI, V) in silicate solutions, Radiochemistry (Moscow), 46, 574-577.

Shvareva, T. Y., Mazeina, L., Gorman-Lewis, D., Burns, P. C., Szymanowski, J. E. S., Fein, J. B., Navrotsky, A., 2011. Thermodynamic characterization of boltwoodite and uranophane: Enthalpy of formation and aqueous solubility, Geochim. Cosmochim. Acta 75, 5269–5282.

SKB. 2011. Long-term safety for the final repository for spent nuclear fuel at Forsmark, Main report of the SR-Site project, SKB TR-11-01, Svensk Kärnbränslehantering AB, Stockholm.

Stanley, D. M., Wilkin, R.T., 2019. Solution equilibria of uranyl minerals: Role of the common groundwater ions calcium and carbonate. Journal of Hazardous Materials, 377, 315-320

Stockmann, M., Schikora, J., Becker, D.-A., Flügge, J., Noseck, U., Brendler, V., 2017. Smart K_d-values, their uncertainties and sensitivities – Applying a new approach for realistic distribution coefficients in geochemical modeling of complex systems. Chemosphere 187, 277-285.

Thakur, P., Singh, D.K., Choppin, G.R., 2007. Polymerization study of *o*-$Si(OH)_4$ and complexation with Am(III), Eu(III) and Cm(III). Inorg. Chimica Acta, 360, 3705–3711.

Thoenen T., Hummel W., Berner U., Curti E., 2014. The PSI/Nagra Chemical Thermodynamic Database 12/07, PSI Report 14-04

Xu, Z.; Sun, Y.; Niu, Z.; Xu, Y.; Wei, X.; Chen X.; Pan, D.; Wu, W. 2020. Kinetic determination of sedimentation for GMZ bentonite colloids in aqueous solution: Effect of pH, temperature and electrolyte concentration. Applied Clay Science, 105393

Yalcintas, E., 2016. Redox, solubility and sorption chemistry of technetium in dilute to concentrated saline systems, Ph.D. thesis.

Yusov, A. B., Fedoseev, A. M., Isakova, O. V., Delegard, C. H., 2005. Complexation of Np(V) with silicate ions, Radiochemistry (Moscow), 47, 39-44.

Appendix

The appendix contains short information and data tables for the reference (BWO, BWR, GGW) and mixed waters (MWR, MWO), A.1., the results of the benchmark calculations (A.2) and the thermodynamic data (A.3) used by Group A and Group B for the elements Th, Am, Se, Tc, U, Np and Pu.

A.1 Reference waters and mixed waters

The data for the reference waters are compiled in Table A.1. Oxidizing conditions – prevailing in the early state of the experiment – and reducing conditions expected to evolve throughout the experiment – are considered.

The charge imbalance in the bentonite porewater was compensated by allowing a slight increase of the chlorine concentration, which has no impact on the radionuclide speciation.

Once suitable charge-balanced waters were defined, the Grimsel groundwater (GGW) was mixed with the bentonite solution. The pH values of the resulting mixtures were predicted by allowing their values to vary under the electrical neutrality constraint. The calculation of the mixed waters results in very similar element concentrations for both Group A and Group B and only slightly differing pH values. With respect to the Eh-value of the waters different approaches were used. For Group A the redox potentials of the resulting mixtures were predicted by allowing their values to vary under the constraint of a constant number of redox electrons. Group B applied Eh values similar to the ones proposed for reducing and oxidizing bentonite porewater to the mixed waters (see *Table A.1*). This results in more reducing conditions for MWR (Eh_{SHE} = -303 mV) and MWO (Eh_{SHE} = -148 mV), for the calculations from Group A compared to the values of Eh_{SHE} = -220 mV and Eh_{SHE} = +100 mV for the calculations from Group B.

Table A.1 pH, Eh values and concentration of dissolved elements in [mol L^{-1}] in bentonite porewater oxidizing, reducing (BPWO,R), Grimsel groundwater (GGW) and mixed waters reducing and oxidizing (MWR, MWO) used by Group A and Group B

	BPWR	BPWO	GGW	Group A		Group B	
				MWR	MWO	MWR	MWO
log pCO_2[a]	-3.5		-	-		-	
pH	7.44		9.6	9.06		8.97	
Eh(SHE. mV)	-200	100	-220	-303	-148	-220	100
Na	$3.3 x 10^{-1}$		$6.9 x 10^{-4}$	$3.39 x 10^{-2}$		$3.46 x 10^{-2}$	
K	$2.6 x 10^{-3}$		$5.0 x 10^{-6}$	$2.65 x 10^{-4}$		$2.72 x 10^{-4}$	
Mg	$8.1 x 10^{-2}$		$6.2 x 10^{-7}$	$8.10 x 10^{-3}$		$8.34 x 10^{-3}$	

Ca	$6.8x10^{-2}$		$1.4\ x10^{-4}$	$6.93\ x10^{-3}$		$7.13\ x10^{-3}$	
Al	-		$2.63\ x10^{-6}$	$2.37\ x10^{-6}$		$2.37\ x10^{-6}$	
Fe	$2.0x10^{-9}$	$1.0x10^{-9}$	$3.0\ x10^{-9}$	$2.91\ x10^{-9}$	$2.80\ x10^{-9}$	$2.91\ x10^{-9}$	$2.80\ x10^{-9}$
Mn	-		$5.0\ x10^{-9}$	$4.50\ x10^{-9}$		$4.50\ x10^{-9}$	
Sr	$6.1x10^{-4}$		$2.0\ x10^{-6}$	$6.28\ x10^{-5}$		$6.28\ x10^{-5}$	
Cl	$4.2x10^{-1}$		$1.6\ x10^{-4}$	$5.95\ x10^{-2}$		$4.34\ x10^{-2}$	
HCO_3[a]	$3.1x10^{-4}$		$4.5\ x10^{-4}$	$4.35\ x10^{-4}$		$4.37\ x10^{-4}$	
Si	$1.8x10^{-4}$		$2.5\ x10^{-4}$	$2.43\ x10^{-4}$		$2.44\ x10^{-4}$	
SO_4	$1.9x10^{-2}$		$6.1\ x10^{-5}$	$1.96\ x10^{-3}$		$2.01\ x10^{-3}$	
F	-		$3.6\ x10^{-4}$	$3.24\ x10^{-4}$		$3.24\ x10^{-4}$	
Br	-		$3.8\ x10^{-7}$	$3.42\ x10^{-7}$		$3.42\ x10^{-7}$	

[a] log pCO_2 = logarithm of CO_2 partial pressure, [b] HCO_3 = total carbonate concentration

A.2. Thermodynamic calculations

A.2.1. Thorium

Table A.2 Solubility limiting phase (SLP), maximum concentration [mol L^{-1}] and fraction of dominating species [%] calculated for thorium. n.d = not in database

	BPWR/BPWO			GGW			MWR/MWO		
	Group A		Group B	Group A		Group B	Group A		Group B
SLP[a]	ThO_2,ag	ThO_2,fr	ThO_2,fr	ThO_2,ag	ThO_2,fr	ThO_2,fr	ThO_2,ag	ThO_2,fr	ThO_2,fr
Th_{tot}	$1.69x10^{-9}$	$1.1x10^{-8}$	$1.4x10^{-8}$	$2.4x10^{-9}$	$1.5x10^{-8}$	$1.5x10^{-8}$	$2.2x10^{-9}$	$1.5x10^{-8}$	$1.4x10^{-8}$
$Th(OH)_4$	69	69	59	52	52	53	58	58	53
$Th(OH)_3^+$	n.d.	n.d.	8	n.d.	n.d.	<1	n.d.	n.d.	<1
$Th(OH)_2(CO_3)$	1	1	1	<1	<1	<1	<1	<1	<1
$Th(OH)_3(CO_3)^-$	28	28	30	45	45	44	39	39	44
$Th(OH)_2(CO_3)_2^{2-}$	1	1	2	3	3	3	3	3	3

[a] ag = aged and fr = fresh

A.2.2. Americium

Table A.3 Solubility limiting phase (SLP), maximum concentration and [mol L^{-1}] and fraction of dominating species [%] calculated for americium

	BPWR/BPWO		GGW		MWR/MWO	
	Group A	Group B	Group A	Group B	Group A	Group B
SLP	$Am(CO_3)(OH)$ (am)	$Am(CO_3)(OH)$ (am)	$Am(OH)_3$ (am)	$Am(OH)_3$ (am)	$Am(CO_3)(OH)$ (am)	$Am(CO_3)(OH)$ (am)
Am_{tot}	4.0×10^{-5}	2.4×10^{-5}	8.7×10^{-8}	5.0×10^{-8}	6.8×10^{-7}	3.1×10^{-7}
Am^{3+}	4	12	<1	<1	<1	<1
$Am(OH)_2^+$	<1	<1	<1	<1	1	3
$Am(OH)^{2+}$	2	5	19	33	9	18
$Am(OH)_3$	<1	<1	<1	1	<1	<1
$Am(CO_3)^+$	8	12	10	13	10	21
$Am(CO_3)^{2-}$	<1	<1	50	43	10	12
$Am(SO_4)^+$	1	4	<1	<1	<1	<1
$AmCl^{2+}$	<1	1	<1	<1	<1	<1
$AmOSi(OH)_3^{2+}$	83	64	20	9	70	46

A.2.3. Selenium

Table A.4 Solubility limiting phase (SLP), maximum concentration [mol L^{-1}] and fraction of dominating species [%] calculated for selenium. n.c.: not considered in calculations

	BPWR		BPWO		GGW		MWR		MWO	
	Group A	Group B	Group A	Group B	Group A	Group B	Group A	Group B	Group A	Group B
SLP	Se(cr)	Se(s)	Se(cr)	Se(s)	Se(cr)	Se(s)	$FeSe_2$	Se(s)	$FeSe_2$	$Ca(SeO_3) \cdot H_2O(s)$
Se_{tot}	1.0×10^{-8}	6.8×10^{-9}	3.1×10^{-9}	2.5×10^{-9}	2.2×10^{-9}	1.7×10^{-10}	1.7×10^{-8}	8.7×10^{-10}	2.0×10^{-7}	3.7×10^{-4}
HSe^-	90	100	<1	<1	11	100	100	99	<1	<1

Se_4^{2-}	8	n.c	<1	n.c	73	n.c.	<1	n.c.	98	n.c.
Se_3^{2-}	2	n.c	<1	n.c	16	n.c.	<1	n.c.	2	n.c.
$H(SeO_3)^-$	<1	<1	78	70	<1	<1	<1	<1	<1	11
SeO_3^{2-}	<1	<1	22	30	<1	<1	<1	1	<1	89

A.2.4. Technetium

*TableA.5 Solubility limiting phase (SLP), maximum concentration [mol L^{-1}] and fraction of dominating species [%] calculated for technetium. *n.s.l. = not solubility limited*

	BPWR		BPWO		GGW		MWR		MWO	
	Group A	Group B	Group A	Group B	Group A	Group B	Group A	Group B	Group A	Group B
SLP	$TcO_2 \cdot 1.6H_2O(s)$ / $TcO_2 \cdot 1.63H_2O(s)$									
Tc_{tot}	4.1x10^{-9}	4.0x10^{-9}	1.7Ex10^{-3}	1.8x10^{-3}	4.2x10^{-9}	4.3x10^{-9}	4.1x10^{-9}	4.1x10^{-9}	4.9x10^{-9}	n.s.l.*
$TcO(OH)_2$	99	99	<1	<1	94	88	98	15	81	13
$(TcO)(OH)_3^-$	<1	<1	<1	<1	5	12	2	<1	1	<1
TcO_4^-	<1	<1	100	100	<1	<1	<1	84	17	86

A.2.5. Uranium

Table A.6 Solubility limiting phase (SLP), maximum concentration [mol L^{-1}] and fraction of dominating species [%] calculated for uranium; n.d.: not in database

	BPWR		BPWO		GGW		MWR		MWO	
	Group A	Group B	Group A	Group B	Group A	Group B	Group A	Group B	Group A	Group B
SLP	UO2 (am.hyd)	UO2·2H$_2$O (am)	Uranophane		Uranophane		UO_2 (am.hyd)	Uranophane	Uranophane	
U_{tot}	9.1x10^{-9}	3.5 x10^{-8}	8.1 x10^{-8}	7.3x10^{-7}	2.9 x10^{-8}	3.5x10^{-8}	3.2 x10^{-8}	3.5 x10^{-7}	7.5 x10^{-8}	2.1 x10^{-7}
$U(OH)_4$	33	9	<1	<1	<1	<1	10	<1	<1	<1
$UCO_3(OH)_3^-$	27	n.d.	<1	n.d.	<1	n.d.	13	n.d.	<1	n.d.
UO_2^+	5	<1	<1	<1	<1	<1	<1	<1	<1	<1
$UO_2(CO_3)_3^{4-}$	<1	<1	<1	<1	7	5	<1	<1	2	<1

$Ca_2UO_2(CO_3)_3$	14	80	40	89	<1	21	8	80	10	80
$CaUO_2(CO_3)_3^{2-}$	19	9	54	10	91	72	62	20	80	20
$MgUO_2(CO_3)_3^{2-}$	2	n.d.	5	n.d.	<1	n.d.	6	n.d.	8	n.d.

A.2.6. Neptunium

Table A.7 Solubility limiting phase (SLP), maximum concentration [mol L^{-1}] and fraction of dominating species [%] calculated for neptunium; n.d.: not in database

	BPWR		BPWO		GGW		MWR		MWO	
	Group A	Group B	Group A	Group B	Group A	Group B	Group A	Group B	Group A	Group B
SLP	NpO_2(am.hyd) / $NpO_2{\cdot}2H_2O$(am)									
Np_{tot}	$9.9x10^{-10}$	$1.0x10^{-9}$	$6.7x10^{-9}$	$1.9x10^{-9}$	$1.0x10^{-9}$	$1.0x10^{-9}$	$9.9x10^{-10}$	$1.0x10^{-9}$	$1.0x10^{-9}$	$2.5x10^{-9}$
$Np(OH)_4$	98	97	14	52	100	98	100	98	99	40
$Np(OH)_3^+$	2	2	<1	1	<1	<1	<1	<1	<1	<1
$Np(CO_3)(OH)_3^-$	<1	1	<1	<1	<1	2	<1	2	<1	1
NpO_2^+	<1	<1	13	44	<1	<1	<1	<1	<1	30
NpO_2Cl	n.d.	1	n.d.	1	n.d.	<1	n.d.	<1	n.d.	<1
$NpO_2(CO_3)^-$	<1	<1	<1	1	<1	<1	<1	<1	<1	29
$NpO_2SiO(OH)_3$	<1	n.d.	73	n.d.	<1	n.d.	<1	n.d.	1	n.d.

A.2.7. Plutonium

Table A. 8 Solubility limiting phase (SLP), maximum concentration [mol L^{-1}] and fraction of dominating species [%] calculated for plutonium; n.d.: not in database

	BPWR		BPWO		GGW		MWR		MWO	
	Group A	Group B	Group A	Group B	Group A	Group B	Group A	Group B	Group A	Group B
SLP	PuO_2 (hyd, ag)	$Pu(OH)_4$ (am)	PuO_2 (hyd, ag)	$Pu(OH)_4$ (am)	PuO_2 (hyd, ag)	$Pu(OH)_4$ (am)	PuO_2 (hyd, ag)	$Pu(OH)_4$ (am)	PuO_2 (hyd, ag)	$Pu(OH)_4$ (am)
Pu_{tot}	$4.3 x10^{-9}$	$2.9 x10^{-8}$	$3.9 x10^{-11}$	$5.5 x10^{-10}$	$8.2 x10^{-11}$	$5.5 x10^{-10}$	$6.8 x10^{-11}$	$5.0 x10^{-10}$	$6.5 x10^{-11}$	$5.0 x10^{-10}$
Pu^{3+}	3	39	<1	<1	<1	<1	<1	<1	<1	<1

$Pu(OH)^{2+}$	3	22	<1	<1	<1	<1	<1	<1	<1	<1
$Pu(CO_3)^+$	6	12	<1	<1	<1	<1	<1	<1	<1	<1
$Pu(SO_4)^+$	4	22	<1	<1	<1	<1	<1	<1	<1	<1
$Pu(SO_4)_2^-$	<1	3	<1	<1	<1	<1	<1	<1	<1	<1
$PuCl^{2+}$	6	n.d.	<1	n.d.	<1	n.d.	<1	n.d.	<1	n.d.
$PuSiO(OH)_3^{2+}$	77	n.d.	<1	n.d.	<1	n.d.	3	n.d	<1	n.d
$Pu(OH)_4$	<1	2	6	92	3	92	3	100	4	100
$Pu(OH)_3^+$	<1	8	<1	8	<1	8	<1	<1	<1	<1
$Pu(CO_3)(OH)_3^-$	<1	n.d.	94	n.d.	97	n.d.	91	n.d.	96	n.d.

A.3. Thermodynamic data

A.3.1. Thorium

Table A.9 Relevant stability constants logβ and solubility products logK for thorium contained in the databases of Group A and Group B

Species	**Group A**	**Group B**
Th^{4+} + 3 H_2O = **$Th(OH)_3^+$** + 3 H^+	Not in DB[a]	-11
Th^{4+} + 4 H_2O = **$Th(OH)_4$** + 4 H^+	-17.4	-17.40
Th^{4+} + CO_3^{2-} + 2 H_2O = **$Th (CO_3)(OH)_2$** + 2 H^+	2.51	2.50
Th^{4+} + 2 CO_3^{2-} + 2 H_2O = **$Th(CO_3)_2(OH)_2^{2-}$** +2 H^+	8.81	8.80
Th^{4+} + CO_3^{2-} + 3 H_2O = **$Th(CO_3)(OH)_3^-$** + 3 H^+	-3.69	-3.70
Th^{4+}+ CO_3^{2-} + 4 H_2O = **$Th(CO_3)(OH)_4^{2-}$** + 4 H^+	-15.6	-15.60
ThO_2(am,fresh) + 4H^+= Th^{4+} + 2 H_2O	9.3	9.30
ThO_2(am,aged) + 4H^+ = Th^{4+} + 2 H_2O	8.5	8.50

[a] DB = database

A.3.2. Americium

Table A.10 Relevant stability constants logβ and solubility products logK for americium contained in the databases of Group A and Group B. Not in DB = not in database

Species	**Group A**	**Group B**

Am^{3+} + H$_2$O = **AmOH**$^{2+}$ + H$^+$	-7.2	-7.20
Am^{3+} +2 H$_2$O = **Am(OH)**$_2^+$ + 2 H$^+$	-15.1	-15.10
Am^{3+} +3 H$_2$O = **Am(OH)**$_3$ +3 H$^+$	-26.2	-26.20
Am^{3+} + CO$_3^{2-}$ = **AmCO**$_3^+$	8	7.90
Am^{3+} +2 CO$_3^{2-}$ = **Am(CO**$_3$**)**$_2^-$	12.9	12.60
Am^{3+} + Si(OH)$_4$ = **AmSiO(OH)**$_3^{2+}$ + H$^+$	-1.71	-2.31
Am^{3+} + SO$_4^{2-}$ = **AmSO**$_4^+$	3.3	3.45
Am^{3+} + Cl$^-$ = **AmCl**$^{2+}$	0.24	0.24
Am(CO$_3$**)(OH)(am)** + H$^+$= Am^{3+} + CO$_3^{2-}$ + H$_2$O	-6.2	-6.20
Am(CO$_3$**)(OH)(s)** + H$^+$= Am^{3+} + CO$_3^{2-}$ + H$_2$O	Not in DB	-8.40*
Am(OH)$_3$**(am)** + 3 H$^+$= Am^{3+}+ 3 H$_2$O	16.9	16.90

* AmOHCO$_3$·0.5H$_2$O(cr)

A.3.3. Selenium

Table A.11 Relevant stability constants logβ and solubility products logK for selenium contained in the databases of Group A and Group B. Not in DB = not in database

Species	**Group A**	**Group B**
9 H$^+$ +8 e- + SeO$_4^{2-}$ = **HSe**$^-$ + 4 H$_2$O	81.60	81.57
2 H$^+$ +2 e$^-$ + SeO$_4^{2-}$ = **SeO**$_3^{-2}$ + H$_2$O	28.05	28.04
H$^+$ + SeO$_3^{2-}$ = **HSeO**$_3^-$	8.36	8.36
3HSe$^-$ = **Se**$_3^{2-}$ + 3H$^+$ + 4e$^-$	5.24	–[a]
4 HSe- = **Se**$_4^{2-}$ + 4 H$^+$ + 6 e$^-$	13.38	–[a]
FeSe$_2$**(cr)** +2 H$^+$ +2 e = 2 HSe$^-$ + Fe^{2+}	-17.13[b]	-17.13
Se(s) + H$^+$ +2 e$^-$= HSe$^-$	-7.60	-7.62
Fe1.04Se(beta) + H$^+$ = 1.04Fe^{2+} + 0.080e$^-$ + HSe$^-$	Not in DB	-3.40
Ca(SeO3):H2O = Ca^{2+} + SeO$_3^{2-}$ + H$_2$O	-6.40	-6.4

[a] available in database but not used; [b] taken from ThermoChimie database

A.3.4. Technetium

Table A.12 Relevant stability constants logβ and solubility products logK for technetium contained in the databases applied by Group A and Group B. Value in brackets is thermodynamic data for the solid $TcO_2·0.6H_2O(s)$ from THEREDA database (Moog et al. 2015)

Species	**Group A**	**Group B**
$TcO(OH)_2 + H_2O = \mathbf{TcO(OH)}^{3-} + H^+$	-10.9	-10.80
$TcO(OH)_2 + CO_3^{2-} + 2\,H^+ = \mathbf{Tc(CO_3)(OH)_2} + H_2O$	19.30	19.26
$TcO(OH)_2 + H^+ + CO_3^{2-} = \mathbf{Tc(CO_3)(OH)_3}^-$	-11.00	-10.96
$TcO(OH)_2 + H_2O = \mathbf{TcO_4}^- + 4H^+ + 3\,e^-$	-29.40	-29.43
$\mathbf{TcO_2·1.6H_2O(s)} = TcO(OH)_2 + 0.6\,H_2O$	-8.4	-8.40
$\mathbf{TcO_2·0.6H_2O(s)} + 0.4\,H_2O = TcO(OH)_2$	(-8.8)	--

A.3.5. Uranium

Table A.13 Relevant stability constants logβ and solubility products logK for uranium contained in the databases applied by Group A and Group B. Not in DB = not in database

Species	**Group A**	**Group B**
$UO_2^{2+} + 3H_2O = \mathbf{UO_2(OH)_3}^- + 3H^+$	-20.25	-20.25
$UO_2^{2+} + 2H_2O = \mathbf{UO_2(OH)_2} + 2H+$	-12.15	-12.15
$3UO_2^{2+} + 5H_2O = \mathbf{(UO_2)_3(OH)_5}^+ + 5H^+$	-15.55	-15.55
$3UO_2^{2+} + 7H_2O = \mathbf{(UO_2)_3(OH)_7}^- + 7H^+$	-32.2	-32.2
$4UO_2^{2+} + 7H_2O = \mathbf{(UO_2)_4(OH)_7}^+ + 7H^+$	-21.9	-21.9
$UO_2^{2+} + 2CO_3^{2-} = \mathbf{UO_2(CO_3)_2}^{2-}$	16.61	16.61
$UO_2^{2+} + 3CO_3^{2-} = \mathbf{UO_2(CO_3)_3}^{4-}$	21.84	21.84
$2UO_2^{2+} + CO_3^{2-} + 3H_2O = \mathbf{(UO_2)_2(CO_3)(OH)_3}^- + 3H^+$	-0.86	-0.86
$2Ca^{2+} + 3CO_3^{2-} + UO_2^{2+} = \mathbf{Ca_2UO_2(CO_3)_3}$	29.22 (30.6)	30.7
$Ca^{2+} + UO_2^{2+} + 3CO_3^{2-} = \mathbf{CaUO_2(CO_3)_3}^{2-}$	27.18	27.18
$Mg^{2+} + UO_2^{2+} + 3\,CO_3^{2-} = \mathbf{MgUO_2(CO_3)_3}^{2-}$	26.11	Not in DB
$U^{4+} + 3H_2O = \mathbf{U(OH)_3}^+ + 3H^+$	-4.70	-4.70
$U^{4+} + 4H_2O = \mathbf{U(OH)_4} + 4H^+$	-10.0	-10.0
$U^{4+} + CO_3^{2-} + 3\,H_2O = \mathbf{UCO_3(OH)_3}^- + 3\,H^+$	4.0	Not in DB
$4H^+ + UO_2^{2+} + 2e^- = U^{4+} + 2H_2O$	9.04	9.04

$UO_2^{2+} + e^- = UO_2^+$	1.484	1.48
Schoepite: UO_3:$2H_2O$ + $2 H^+ = UO_2^{2+}$ + 3 H2O	5.96	5.96
Becquerelite(nat): $Ca(UO_2)_6O_4(OH)_6$:$8H_2O$ + $14 H^+ = Ca^{2+} + 6 UO_2^{2+} + 18 H_2O$	40.5	29.0
Uranophane: $Ca(H_3O)_2(UO_2)_2(SiO_4)_2$:$3H_2O$ + $6H^+= Ca^{2+} + 2 UO_2^{2+} + 2 Si(OH)_4 + 5 H_2O$	9.42 (10.82)	9.42
UO_2:$2H_2O$(am) + $4 H^+ = U^{4+} + 4 H_2O$	Not in DB	1.5
UO_2(am) + $4 H^+ = U^{4+} +2 H_2O$	1.5	Not in DB

A.3.6. Neptunium

Table A.14 Relevant stability constants logβ and solubility products logK for neptunium contained in the databases of Group A and Group B. Not in DB = not in database

Species	**Group A**	**Group B**
$Np^{4+} +3 H_2O =$ **$Np(OH)_3^+$+3** H^+	-2.8	-2.8
$Np^{4+} +4 H_2O =$ **$Np(OH)_4$** $+4 H^+$	-8.3	-8.3
$Np^{4+} +2 CO_3^{2-} +2 H_2O =$ **$Np(CO_3)_2(OH)_2^{2-}$** $+2 H^+$	Not in DB	15.17
$Np^{4+} + CO_3^{2-} +3H_2O =$ **$NpCO_3(OH)_3^-$** $+3H^+$	2.0	3.82
$Np^{4+} + CO_3^{2-} + 4 H_2O =$ **$NpCO_3(OH)_4^{2-}$** $+ 4 H^+$	Not in DB	-6.83
$NpO_2^{2+} + e^- =$ **NpO_2^+**	19.59	19.59
$NpO_2^+ H_2O =$ **NpO_2OH** $+ H^+$	-11.3	-11.30
$NpO_2^+ + Cl^- =$ **NpO_2Cl**	Not in DB	-0.93
$NpO_2^+ + SiO(OH)_3^- =$ **$NpO_2SiO(OH)_3$**	7.0	Not in DB
NpO_2:$2H_2O$(am) + 4H+ = $Np^{4+} + 4H_2O$	Not in DB	-0.7
NpO_2 (am, hyd) + 4H+= $Np^{4+} + 2H_2O$	-0.7	Not in DB
NpO_2OH(am, fr) + H+ = $NpO_2^+ + H_2O$	5.3	5.3

A.3.7. Plutonium

Table A.15 Relevant stability constants logβ and solubility products logK for plutonium contained in the databases of Group A and Group B. Not in DB = not in database

Species	**Group A**	**Group B**
Pu^{4+} + e^- = **Pu^{3+}**	17.69	17.69
Pu^{3+} + H_2O = **$PuOH^{2+}$** + H^+	-6.9	-6.90
Pu^{3+} + CO_3^{2-} = **$PuCO_3^+$**	8	7.64
Pu^{3+} + 2 CO_3^{2-} = **$Pu(CO_3)_2^-$**	12.9	12.54
Pu^{3+} + SO_4^{2-} = **$PuSO_4^+$**	3.9	3.91
Pu^{3+}+ 2 SO_4^{2-} = **$Pu(SO_4)_2^-$**	5.7	5.70
Pu^{3+} + Cl^- = **$PuCl^{2+}$**	1.2	Not in DB
Pu^{3+} + $Si(OH)_4$ = **$PuSiO(OH)_3^{2+}$** + H^+	-1.71	Not in DB
Pu^{4+} + 4 H_2O = **$Pu(OH)_4$** + 4 H^+	-9.3	-8.50
Pu^{4+} + CO_3^{2-} + 3 H_2O = **$Pu(CO_3)(OH)_3^-$** + 3 H^+	6.0	Not in DB
Pu^{4+}+ 2 CO_3^{2-} + 2 H_2O = **$Pu(CO_3)_2(OH)_2^{2-}$** + 2 H^+	Not in DB	16.76
PuO_2(hyd,ag) + 4 H^+ = Pu^{4+} + 2 H_2O	-2.33	-2.37
$Pu(OH)_4$(am) + 4 H^+ = Pu^{4+} + 4 H_2O	Not in DB	-0.80

CRediT authorship contribution statement

Vanessa Montoya: Investigation, conceptualization, methodology, interpretation, supervision, writing, simulations Group B, review & editing. **Ulrich Noseck**: Investigation, methodology, Writing, simulations Group A. **Felix Mattick**: simulations Group B. **Susan Britz**: simulations Group A, **Ingo Blechschmidt**: review, project management. **Thorsten Schäfer**: Conceptualization, writing, Funding acquisition

Declaration of Competing Interest

☒ The authors declare that they have no known competing financial interests or personal relationships that could have appeared to influence the work reported in this paper.

☐The authors declare the following financial interests/personal relationships which may be considered as potential competing interests:

Highlights

- Benchmarking models to understand radionuclides behaviour in repository systems
- Chemical thermodynamic data in support of deep geological repositories is essential
- Se, Tc, U, Np, Am, Pu and Th (as analog of tetravalent actinides) are investigated
- Relevant geochemical data and gaps identified to predict radionuclide migration
- The model support an in-situ experiment within a shear zone in a crystalline rock